LBL-8730
Vol. I

HEATER TEST PLANNING FOR THE NEAR SURFACE TEST FACILITY AT THE HANFORD RESERVATION

BY

A. DuBois, E. Binnall, T. Chan,
M. McEvoy, P. Nelson, and J. Remer

Earth Sciences Division
Lawrence Berkeley Laboratory
University of California
Berkeley, California 94720

VOLUME I
TABLE OF CONTENTS

		Page
List of Figures		v
List of Tables		vii
I.	INTRODUCTION	1
II.	EXPERIMENT DESIGN AND PROCEDURES--P. Nelson	3
III.	THERMO-MECHANICAL MODELING--T. Chan and J. Remer	6
	Physical Systems to be Modeled	7
	Full-Scale Heater Experiments	7
	Time-Scaled Heater Experiment	10
	Thermal and Thermo-mechanical Models Used	14
	Closed Form Integral Solutions for Thermal Analysis	14
	Finite Element Thermo-mechanical Models	17
	Results and Discussion	19
	Full-Scale Experiments	19
	Time-Scaled Experiment	41
	Recommendations	41
IV.	HEATER AND ROCK INSTRUMENTATION LAYOUT--A. DuBois	44
V.	HEATERS AND CONTROLS--E. Binnall and A. DuBois	45
	Full-Scale Heater.	46
	Time Scaled Heaters	59
	Auxiliary Systems	62
	Electrical Heater Controllers	70
VI.	INSTRUMENTATION AND DATA ACQUISITION SYSTEM--M. McEvoy and E. Binnall.	74
VII.	REFERENCES	80

VOLUME II
TABLE OF CONTENTS

Page

1. Theoretical Support for Radioactive Waste Storage Projects: Development of Data Analysis Methods and Numerical Models-- C. F. Tsang and T. Chan..... 1-1
2. Injectivity Temperature Profiling as a means of Permeability Characterization -- P. Nelson..... 2-1
3. Geophysical Holes at NSTF, Hanford -- P. Nelson, T. Doe and H. Pratt..... 3-1
4. Proposed Geophysical and Hydrological Measurements at NSTF, Hanford -- P. Nelson and T. Doe..... 4-1
5. Suggestions for Characterization of the Discontinuity System at NSTF, Hanford -- R. Thorpe..... 5-1
6. Monitoring Rock Property Changes Caused by Radioactive Waste Storage Using the Electrical Resistivity Method -- H. F. Morrison..... 6-1
7. Microseismic Detection System for Heated Rock -- M. S. King..... 7-1
8. Pasco Basin Groundwater Contamination Study -- D. Girvin..... 8-1
9. Letter to Mark Board on Gable Mountain Faulting -- H. Wollenberg..... 9-1
10. Report on Hydrofracturing Tests for In Situ Stress Measurement, Near Surface Test Facility, Hole DC-11, Hanford Reservation -- B. C. Haimson..... 10-1
11. Borehole Instrumentation Layout for Hanford Near Surface Test Facility -- Terra Tek..... 11-1

VOLUME I
TABLE OF CONTENTS

		Page
List of Figures		v
List of Tables		vii
I.	INTRODUCTION	1
II.	EXPERIMENT DESIGN AND PROCEDURES--P. Nelson	3
III.	THERMO-MECHANICAL MODELING--T. Chan and J. Remer	6
	Physical Systems to be Modeled	7
	Full-Scale Heater Experiments	7
	Time-Scaled Heater Experiment	10
	Thermal and Thermo-mechanical Models Used	14
	Closed Form Integral Solutions for Thermal Analysis	14
	Finite Element Thermo-mechanical Models	17
	Results and Discussion	19
	Full-Scale Experiments	19
	Time-Scaled Experiment	41
	Recommendations	41
IV.	HEATER AND ROCK INSTRUMENTATION LAYOUT--A. DuBois	44
V.	HEATERS AND CONTROLS--E. Binnall and A. DuBois	45
	Full-Scale Heater	46
	Time Scaled Heaters	59
	Auxiliary Systems	62
	Electrical Heater Controllers	70
VI.	INSTRUMENTATION AND DATA ACQUISITION SYSTEM--M. McEvoy and E. Binnall	74
VII.	REFERENCES	80

VOLUME II
TABLE OF CONTENTS

Page

1. Theoretical Support for Radioactive Waste Storage Projects: Development of Data Analysis Methods and Numerical Models-- C. F. Tsang and T. Chan..... 1-1
2. Injectivity Temperature Profiling as a means of Permeability Characterization -- P. Nelson..... 2-1
3. Geophysical Holes at NSTF, Hanford -- P. Nelson, T. Doe and H. Pratt..... 3-1
4. Proposed Geophysical and Hydrological Measurements at NSTF, Hanford -- P. Nelson and T. Doe..... 4-1
5. Suggestions for Characterization of the Discontinuity System at NSTF, Hanford -- R. Thorpe..... 5-1
6. Monitoring Rock Property Changes Caused by Radioactive Waste Storage Using the Electrical Resistivity Method -- H. F. Morrison..... 6-1
7. Microseismic Detection System for Heated Rock -- M. S. King..... 7-1
8. Pasco Basin Groundwater Contamination Study -- D. Girvin..... 8-1
9. Letter to Mark Board on Gable Mountain Faulting -- H. Wollenberg..... 9-1
10. Report on Hydrofracturing Tests for In Situ Stress Measurement, Near Surface Test Facility, Hole DC-11, Hanford Reservation -- B. C. Haimson..... 10-1
11. Borehole Instrumentation Layout for Hanford Near Surface Test Facility -- Terra Tek..... 11-1

LIST OF FIGURES

		Page
Figure 1.	Hanford Full-Scale Experiment.	8
Figure 2.	Power Schedules 1a and 2c.	9
Figure 3.	Hanford Time-Scale Experiment.	12
Figure 4.	Power Schedule 3.	13
Figure 5.	Temperature Profiles for Hanford Full-Scale Experiment, R = 0.203 to 0.881 m.	20
Figure 6.	Temperature Profiles for Hanford Full-Scale Experiment, R = 0.919 to 5.0 m.	21
Figure 7.	Isotherms in Vertical Plane, Hanford Full-Scale Experiment.	25
Figure 8.	Displacement Profile for Mesh 1, Hanford Full-Scale Experiment.	27
Figure 9.	Displacement Profile for Mesh 7, Hanford Full-Scale Experiment.	28
Figure 10.	Hanford Full-Scale Experiment--Deformation of Drift and Borehole.	32
Figure 11.	Stress Profiles for Mesh 1, Hanford Full-Scale Experiment.	33
Figure 12.	Interference Between the Two Full-Scale Experiments --Temperature Profiles.	38
Figure 13.	Interference Between the Two Full-Scale Experiments --Displacement Profiles.	39
Figure 14.	Interference Between the Two Full-Scale Experiments --Stress Profiles.	39
Figure 15.	Isotherms in Horizontal Plane--Hanford Time-Scale Experiment.	42
Figure 16.	Full-Scale Heater Installation in a) Unlined Borehole, b) Lined Borehole.	48
Figure 17.	Full Scale Canister Assembly Ready for Lowering Into a Borehole.	49
Figure 18.	Partial Section Through a Full Scale Heater Canister.	50
Figure 19.	Typical Heating Element Connection in a) Bare Connection, b) Insulated Connection.	53

LIST OF FIGURES (Continued)

Page

Figure 20. Full-Scale Heater Stem Showing Mounting of the Upper Stem and Shroud. 55
Figure 21. Details of Heat Plug for Full Scale Heater. 57
Figure 22. Peripheral Heater Installation. 58
Figure 23. Time Scale Heater Installation. 60
Figure 24. Portable Thermocouple Probe. 65
Figure 25. Schematic of Dewatering Pump Installation. 67
Figure 26. Caliper Assembly Installed in the Time Scale Heater Borehole. 68
Figure 27. Weighing Pan Assembly Installed on the Time Scale Heater. . . 69
Figure 28. Proposed Data Acquisition System Configuration. 77

LIST OF TABLES

		Page
Table 1a.	Dimensions of the full-scale heater experiments.	7
Table 1b.	Power levels of central heater for first two years of the full scale experiment.	10
Table 2.	Material properties used.	14
Table 3.	Calculated temperature rise (^{o}C) at the end of the first, second, and third years of the full scale experiment.	23
Table 4.	Significant temperature values and predicted times at which the temperature is attained.	24
Table 5.	Maximum predicted radial displacement in the midplane.	29
Table 6.	Maximum predicted vertical displacements and the value of z at which the maximum displacements occur.	30
Table 7.	Maximum predicted vertical displacement 0.375 m below the floor of the heater drift.	31
Table 8.	Maximum predicted compressive stresses in the heater midplane.	35
Table 9.	Maximum predicted stresses (σ_r, σ_θ) 0.375 m below the floor of the heater drift.	36
Table 10.	Predicted combined radial displacements in heater midplane of the two full-scale experiments.	40
Table 11.	Lead wire voltage drop.	54
Table 12.	Heater element operating power and voltage.	70

FOREWORD

This report has two parts. Volume I contains the text of the report, and Volume II contains the Appendix. The Appendix is being published under separate cover.

I. INTRODUCTION

An underground test facility is being constructed at Gable Mountain on the Hanford Reservation, Hanford, Washington. The Near Surface Test Facility (NSTF) is the site for a group of experiments designed to evaluate the thermo-mechanical suitability of a deep basalt stratum as a permanent repository for nuclear waste.

The nuclear waste is assumed to be packaged in cylindrical metal canisters which would be lowered into holes bored into a mine floor. Heat is generated in such containers as a result of the continuing decay of radioactive waste. One phase of the NSTF experimental program will evaluate the thermo-mechanical response of the surrounding rock mass to this predictable heat flux.

LBL Earth Science Division was asked to assist Rockwell Hanford Operations (RHO) in designing suitable thermo-mechanical tests for the NSTF because of the division's background in the field of rock mechanics and its experience in designing and executing a similar group of cooperative Swedish-American experiments at the Stripa iron mine in Sweden. After consultations with LBL's Earth Science Division and Terra Tek (a subcontractor to LBL), a test plan titled "Near Surface Test Facility (NSTF) Test Plan" was published by RHO in December 1977 by Board and Marron. As a result of continuing discussions, this preliminary plan has been modified in the ensuing months. The latest version of the plan is an unpublished working document titled "In Situ Heater Experiment Plan" dated July 1978. On September 22, 1978, RHO representatives indicated that they planned to substantially reduce the number of heaters and the amount of rock instrumentation to be used in the tests. Subsequently, LBL and RHO consultations were held to discuss a test plan that would be compatible with these reductions. At present there is no available up-to-date version of a compatible test plan for LBL comment. Therefore the following remarks will not reflect this latest change.

LBL, and their subcontractor Terra Tek, Inc. of Salt Lake City, produced a borehole and instrumentation array for the three proposed heater tests which have been identified as Full Scale Test #1 (lined borehole), Full Scale Test #2 (unlined borehole), and Time Scale Test. LBL has performed thermo-mechanical modeling to help design the three instrumentation arrays and predict the thermal environment of the heaters and instruments. The modeling reported here does not reflect the recent RHO revisions to the "In Situ Heater Experiment Plan." Heaters, instrumentation, and data acquisition system designs and recommendations

were adapted from those used in Sweden. Drawings and specifications were provided for the RHO design of the NSTF drifts and services, and RHO designs and specifications were reviewed. A quality assurance plan was developed, and a program schedule, compatible with earlier assumptions regarding LBL conduct of the tests, was prepared. Component procurement and fabrication planning was started through LBL purchasing and shops, but no formal plan was completed. A year-end summary report was drafted describing the LBL effort and recommended designs.

II. EXPERIMENT DESIGN AND PROCEDURES
P. Nelson

The experimental activities in a facility such as the NSTF are divided into two parts for purposes of this discussion. The first set of activities -- geological, geotechnical, and geophysical -- are primarily carried out before the rock instrumentation is installed into the boreholes and the heater experiments are started. These activities have a number of objectives, including: the definition of the three-dimensional fracture network in the vicinity of the heaters, the spatial distribution of permeability and porosity and their quantification insofar as possible; the mapping of changes in physical properties of the rock which may provide insight into its behavior during thermal loading; and assessment of different techniques in delineating the fracture system in the basalt.

The second set of activities is the operation of the heater tests, including the installation, calibration, check-out, operation, maintenance, and acquisition of data. Among the objectives of the heater tests are:

(1) To investigate canister retrievability.

(2) To measure borehole decrepitation as a function of power level.

(3) To observe temperature and displacement fields and compare the measured levels with predicted levels.

(4) To examine the effects of fractures and jointing on the thermo-mechanical properties.

(5) To assess the long-term response and interaction of an array of storage holes.

It is not possible to document here all the considerations involved in formulating the plans and specifications of the geotechnical and heater studies. As mentioned in the introduction, the planning relied heavily upon the procedures and design adopted for the Stripa project (Witherspoon and Degerman, 1978). Below, the more salient considerations are outlined with reference to pertinent publications and internal memoranda.

(1) Core logging and core photography. Kurfurst, et al. (1978) detail the procedures used on the Stripa project to log and photograph the core after it was recovered from the core barrel. They also explain the precautions taken in the drilling process to ensure good core recovery and quality. No substantial modifications to this procedure were planned for Hanford.

(2) Television borehole logging. Considerable experience with different systems was obtained at Stripa, where fracture aperture, fracture location, and orientation were mapped with three-borehole television systems and compared with the core logging results. No system had yet been specified for Hanford.

(3) Geophysical borehole logging. A commercial logging system was purchased by LBL, modified for underground usage, and used at Stripa (Nelson, 1977). It was anticipated that this same system would be used at Hanford. Tools available include caliper, temperature, neutron, gamma-gamma, and natural gamma. It was also anticipated that development work would continue on a clamped, acoustic tool used at Stripa to measure compressional- and shear-wave velocities for the detection of open cracks.

(4) Air injection permeability. As outlined by Nelson and Doe (1978), an air injection-packer system was seen as the more practical approach to mapping permeability and its variations in the heater test area.

(5) Characterization of fracture discontinuities. Thorpe (1978) presents a detailed and systematic approach to mapping and characterizing fractures.

Other subsidiary measurements that were carried out at Stripa were also planned for Hanford. These include the in situ measurement of modulus by Terra Tek and overcoring measurements for stress (Carlsson, 1978).

The above listing constitutes most of the planned effort prior to the operation of the heater test; the two items below discuss briefly the instrumentation and design consideration for the heater tests.

(1) Thermal and mechanical measurements. Most of the instruments around the two full-scale and time-scale heaters are thermocouples, linear extensometers, and borehole deformation gauges. A draft scope-of-work document has been prepared for the design and installation of these instruments. The fundamental considerations governing the overall design of the Stripa tests are discussed by Cook and Witherspoon (1978). The specifics of the design were altered for the NSTF at Hanford based on two considerations. First, the thermal conductivity is considerably lower in basalt, dramatically altering the predicted thermal field (see subsequent section on thermo-mechanical modeling); second, the assumption of isotropy has been relaxed at Hanford and additional boreholes added to detail any departure from aximuthal symmetry. The resulting borehole layout is discussed in the next section.

(2) Geophysical and hydrological monitor measurements. A memorandum by Nelson and Doe (1978) outlined five types of measurements to be made during

the heater tests. These measurements, which are listed below with pertinent references, are designed to assess changes in the rock mass during the heater tests. In their design it was taken into account that in the future we will need a reliable method of monitoring rock mass behavior in an operating repository.

(a) Measurement of open borehole sequence: air permeability, acoustic velocity, and neutron measurements of water content.

(b) Measurement of acoustic emission: a report by M. King (1978), a consultant, presents a preliminary design, borehole configuration, and cost estimate for a twelve transducer system with pre-processing.

(c) Monitoring of acoustic velocity: considerations by R. Lingle (P.C.) led to the layout of three boreholes in the time scale drift and three in the larger of the two full-scale heaters.

(d) Measurement of electrical resistivity: a proposal by F. Morrison (1978) resulted in the layout of ten shallow, collinear holes for electrodes to be placed down the axis of the large full-scale heater.

(e) Measurement of radio-frequency electromagnetic propagation: no design work for this test has been done, but two boreholes were specified in the full scale heater test for this purpose.

III. THERMO-MECHANICAL MODELING

T. Chan and J. S. Remer

Introduction

The work reported here includes thermal calculations for the full scale and time scaled heater experiments in the Near Surface Test Facility (NSTF) (Rockwell Hanford Operations, 1978) using closed-form integral solutions and thermo-mechanical calculations for the full scale experiments using continuum finite-element models.

The purpose of these calculations is to provide predicted temperatures, displacements, and stresses to be used in the design and layout of heaters and measuring devices and to help in choosing suitable power schedules*. In the context of high-level radioactive waste (reprocessed or unreprocessed spent fuel) storage, both the thermal and the thermo-mechanical responses of the rock to the radioactive decay heat of the waste are of crucial importance. Because of the very long duration that the waste will remain toxic, it is necessary to rely upon mathematical models to make long-term predictions. However, geologic systems are very complicated and any model must be validated by in situ experiments. These experiments would, in turn, reveal the essential features that must be included in the models. Thus, both the calculations presented here and the experiments being modeled should be viewed as part of an iterative process aimed at solving the problem of radioactive waste storage.

Temperatures have been calculated using a closed-form finite line-source solution coded into a computer program FILINE, which has been applied previously to predict the rock temperatures in heater experiments at Stripa (Chan, et al., 1978). It is believed to be the only set of predicted temperatures to-date that has been stored in an onsite computer for real-time comparison with field data from an in situ underground experiment. Excellent agreement has been found between measured (Cook and Hood, 1978) and predicted temperatures. This gives us confidence in using the same program to calculate the temperatures for the NSTF heater experiments which are patterned after the Stripa project (Cook and Witherspoon, 1978).

Detailed results, as well as the development of equations for arbitrary time-dependent finite-cylinder and disc sources and generalization to an anisotropic medium, are given in a separate report (Chan and Remer, 1978a).

---

*The results contained in this report do not reflect the latest design changes which were made in September and October 1978 after the completion of this set of calculations.

Physical Systems to be Modeled

The heater experiments to be modeled consist of two full-scale tests and a time scaled test, essentially an adaptation of the concept used in the Stripa Heater Project (Cook and Witherspoon, 1978). A brief description of the heater arrangements is given below. Further details can be found in the "In Situ Heater Experiment Plan" (unpublished working document, Rockwell Hanford Operations).

Full-Scale Heater Experiments

Each full scale experiment consists of a central heater surrounded by a ring of eight peripheral heaters. This is illustrated schematically in Figure 1, which also shows the cylindrical coordinate system used in the calculations. This heater array is placed into holes drilled from the floor of the heater drift so that the mid-plane of the heaters is approximately 14 feet (4.25 m) below the floor. The central heater simulates the local thermo-mechanical effects of a waste canister, and the peripheral heaters simulate the rise of ambient temperature caused by other canisters in a repository. Dimensions of the heaters and holes are given in Table 1a.

TABLE 1a. Dimensions of the full-scale heater experiments.

	ft/in.		m
Length of central heater canister	8.5	ft	(2.59)
Length of heater element	8.0	ft	(2.44)
Diameter of central heater canister	12.75	in.	(0.324)
Diameter of central heater hole	18.0	in.	(0.457)
Length of peripheral heater	14.0	ft	(4.27)
Diameter of peripheral heater hole	3.0	in.	(0.038)
Radius of the ring of peripheral heaters	35.4	in.	(0.90)
Center to center separation between the two experiments	69.9	ft	(21.00)

Six different power levels and schedules have been considered in the thermal calculations to bracket all reasonable possibilities. The highest and lowest power schedules are illustrated in Figures 2a and 2b. The power schedule of the central heater is best described as a series of step functions, whereas the power output of the peripheral heaters is constant for the whole time of operation.

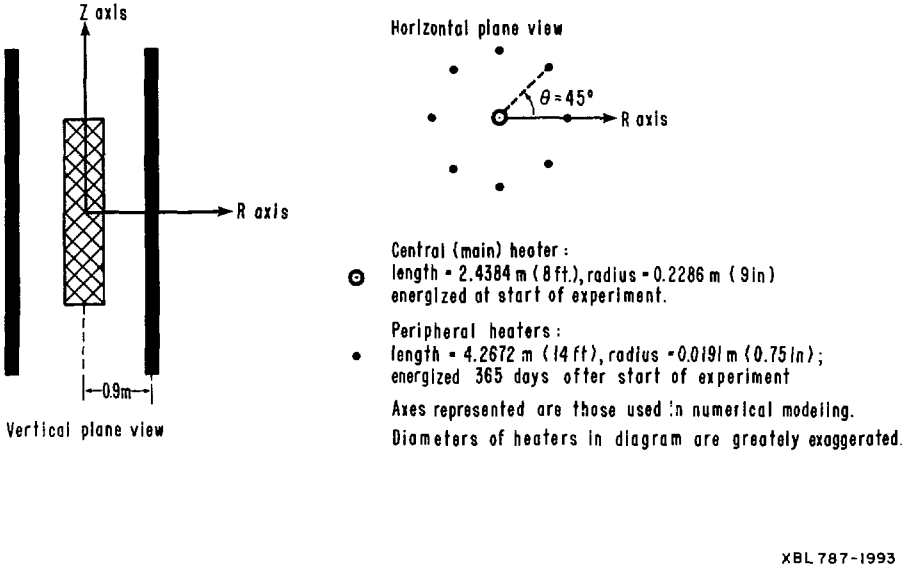

Figure 1. Hanford Full-Scale Experiment.

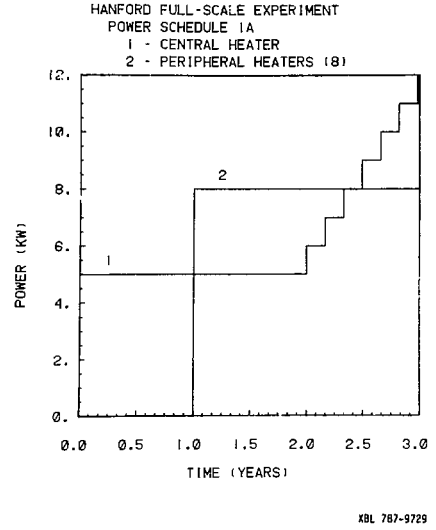

(a)

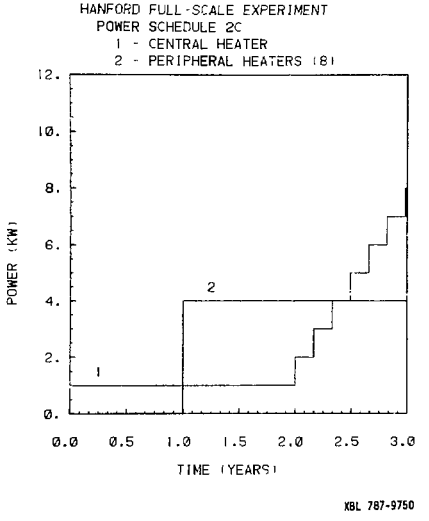

(b)

Figure 2. Power Schedules 1a and 2c.

The power schedules have been divided into two groups based on the power level of the central heater. The central heater for power schedules in the first group (1a, 1b, 1c) has an initial power of either 5 kW or 2.5 kW, and the central heater in the second group has an initial power of either 2 kW or 1 kW. The power levels of the main heater for the first two years of the experiment are given below.

TABLE 1b. Power levels of central heater for first two years of the full scale experiment.

	Power (kW)	
	0 to 180 days	180 to 730 days
Power Schedule 1a	5	5
Power Schedule 1b	2.5	5
Power Schedule 1c	2.5	2.5
Power Schedule 2a	2	2
Power Schedule 2b	1	2
Power Schedule 2c	1	1

The peripheral heaters are energized one year after the experiment is started and their power levels are held constant at either 0.5 kW per peripheral heater (1b, 1c, 2b, 2c) or 1 kW per peripheral heater (1a, 2a).

After the experiments have been running for two years, the overload test will begin. In this test the power level of the central heater is increased by 1 kW every 60 days until the end of the experiment one year later. At the end of three years the highest central-heater power level is 12 kW for power schedule 1a (Figure 2a), and the lowest is 8 kW for schedule 2c (Figure 2b).

Time-Scaled Heater Experiment

The time scaled experiment will simulate the interaction between adjacent nuclear-waste canisters in a row and the interaction between rows in different storage tunnels in a repository for a period approximately equivalent to 30 years of repository operation time. This concept of scaling is based on the laws of linear heat conduction which allow the time to be scaled down by a ratio of linear dimensions. To understand the basis of scaling, one can either examine the solutions (Cook and Witherspoon, 1978) or go to the heat diffusion equation itself. Thus, for simplicity, consider the one-dimensional homogeneous heat diffusion equation:

$$\frac{\partial T}{\partial t} = \kappa \frac{\partial^2 T}{\partial x^2} \tag{1}$$

where:

T = temperature

t = time

x = distance

κ = thermal diffusity.

The solution of Equation (1), T(x,t), gives the temperature distribution of a physical system (I) with spatial variable x and time variable t. Suppose one now has a physical system (II) described by spatial variable $x_d = \frac{x}{L}$ and time variable $t_d = \frac{t}{L^2}$ where L is some scale length. In this case the temperature distribution $T(x_d,t_d)$ of this system satisfies the equation

$$\frac{\partial T}{\partial t_d} = \kappa \frac{\partial^2 T}{\partial x_d^2} . \tag{2}$$

Since equations (1) and (2) are identical, $T(x_d,t_d)$ for system II is equal to T(x,t) for system I.

The time scaled experiment, shown in Figure 3, consists of a rectangular array of nine primary heaters at spacings of 3 m and 7 m with four additional secondary heaters as shown. The mid-plane of this array is 10 m below the floor of the drift. Each heater is 2.66 ft (0.81 m) in length. Comparing with the full scale heater length gives a linear-scale ratio of approximately 1:3.2 and a time scale ratio of approximately 1:10.2. To simulate the effects of sequential step loading, the secondary heaters will be turned on two years after the primary array. This power schedule is referred to as Power Schedule 3, Figure 4. Initial power will be 1.125 kW, which corresponds to a full-scale heater power of 3.6 kW. This represents a 1.5-year-cooled PWR spent fuel assembly. In the preliminary calculations, the power of the heaters has been assumed to be constant. The intention was to decay the power in later calculations according to the expected time variation of the spent-fuel heat-production rate.

Material properties of the host rock, Pomona basalt, are taken from laboratory measurements on small specimens (Martinez-Baez and Amick, 1978) for the thermal calculations and from mean literature values summarized by Agapito

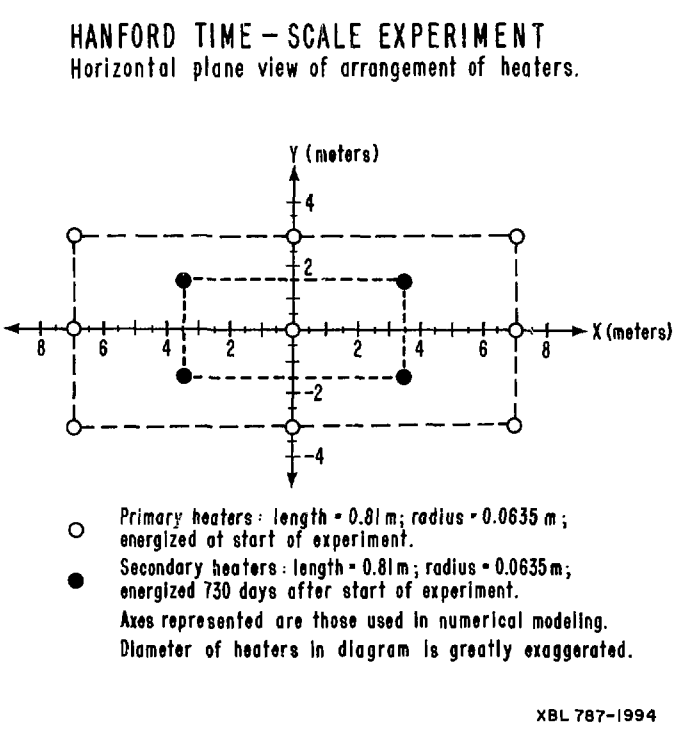

Figure 3. Hanford Time-Scale Experiment.

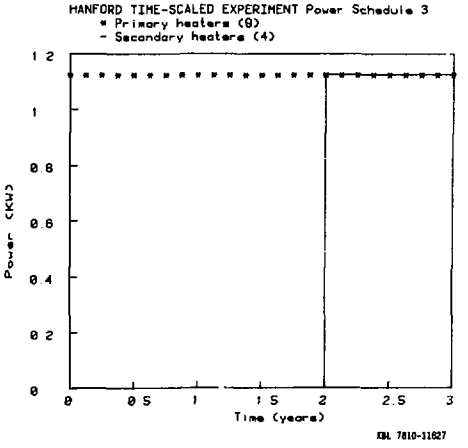

Figure 4. Power Schedule 3.

et al. (1978) for the thermo-mechanical calculations. These are listed in Table 2.

TABLE 2. Material properties used.

Property	Symbol	Value
Density[1]	ρ	2865 kg/m^3
Specific Heat[1]	c	1164 J/kg^oC
Thermal Conductivity[1]	k	1.62 W/m^oC
Thermal Diffusivity[1]	$\kappa = \frac{kc}{\rho}$	$4.86 \times 10^{-7} m^2/sec$
Poisson's Ratio[2]	ν	0.26
Thermal Expansion Coefficient[2]	α	$5.4 \times 10^{-6}/^oC$
Young's Modulus[2]	E	7×10^4 MPa

[1]Values used are "estimated thermal values at 200°C for Pomona basalt" based on laboratory measurements at lower temperatures (Martinez-Baez and Amick, 1978).

[2]Average basalt properties (Agapito et al., 1978). Laboratory data for Pomona basalt (Duvall et al., 1978) was not yet available at the beginning of the present calculation. The elastic properties used are very similar to those measured by Duvall et al., while the thermal expansion coefficient is slightly lower than their laboratory result ($6.6 \times 10^{-6}/^oC$). This laboratory value for the thermal expansion coefficient will lead to proportionally higher thermal stresses and displacements.

Thermal and Thermo-Mechanical Models Used

Closed-Form Integral Solutions for Thermal Analysis

The Green's function method (Morse and Feshbach, 1953) has been used to obtain closed-form integral solutions to the heat transfer problem for the heater experiments. Here the term Green's function is used as it is in applied mathematics, i.e., it includes the point-source method (also known as singularity solution or impulse response) as well as boundary integrals. This technique for solving nonhomogeneous linear partial-differential equations is well known among mathematical physicists and engineers and has been applied to a wide variety of physical problems ranging from electrostatics (Jackson, 1973) to wave propagation (Morse and Feshbach, 1953), heat diffusion (Carlsaw and Jaeger, 1959), and quantum statistical mechanics of electron states in liquid metals (Chan and Ballentine, 1971).

The physical situation in the heater experiments is amenable to this method of solution with the following assumptions:

(1) Conduction is the only mode of heat transfer.

(2) The heaters and the rock medium are both homogeneous, isotropic, and have the same constant (temperature-independent) thermal properties.

(3) The heaters are in direct thermal contact with the rock.

(4) The rock medium can be considered infinite with uniform initial temperature or semi-infinite with the heater drift idealized as an isothermal or adiabatic boundary.

Under these assumptions the problem can be handled with the point-source method, a particular case of the Green's function method.

Due to the short thermal-diffusion time across the radius of the heater and its small heat capacity compared with that of the rock volume to be heated, the heater can be represented by a finite line source. The validity of the assumption has been verified by numerical comparison of the finite line source solution with the finite-cylinder source solution (Chan, et al., 1978). The temperature rise ΔT at a point (x,y,z) at time t due to a line source of power-per-unit length Q_ℓ and length 2b located along the z-axis with its mid-point at the origin can be shown (Chan, et al., 1978) to be:

$$\Delta T(x,y,z,t) = \frac{1}{8\pi k} \int_0^t Q_\ell(t-\mu) \left[\text{erf} \left\{ \frac{z+b}{2(\kappa\mu)^{1/2}} \right\} - \text{erf} \left\{ \frac{z-b}{2(\kappa\mu)^{1/2}} \right\} \right] \times \frac{1}{\mu} \exp\left(\frac{-r^2}{4\kappa\mu}\right) d\mu. \qquad (3)$$

where

$r^2 = x^2 + y^2$,

k = thermal conductivity,

κ = thermal diffusivity.

Similar integral solutions for a finite cylinder source and a disc source are given in Appendix A of Chan and Remer (1978a). Appendix B of that report contains a brief discussion of the generalization of these solutions to an anisotropic medium.

The effect of a plane adiabatic or isothermal boundary can be simulated with positive or negative images, respectively. The total temperature rise

due to an array of N parallel-line heaters in a semi-infinite medium can be obtained by superimposing the temperature rise caused by each, giving

$$\Delta T_{total}(x,y,z,t) = \sum_{h=1}^{N} \Delta T_h(r_h, z-z_h, t-t_h \mid Q_h, b_h) + \sum_{h=1}^{N} \Delta T_h(r_h, z-2z_o + z_h, t-t_h \mid \pm Q_h, b_h) \qquad (4)$$

where

T_h = temperature rise due to the h^{th} heater,

$2b_h$ = length of the h^{th} heater,

Q_h = power-per-unit length of the h^{th} heater,

(x_h, y_h, z_h) = coordinates of the mid-point of the h^{th} heater,

$r_h^2 = (x-y_h)^2 + (y-y_h)^2$,

t_h = turn-on time of the h^{th} heater,

z_o = elevation of the plane boundary,

and all the heaters are oriented parallel to the z-axis. In the case of an infinite medium, only the first term of Equation (4) needs to be considered. For all the three heater experiments being modeled, z_h = o for all heaters.

In the case of the full scale experiments, temperatures were calculated for the various power schedules for both the infinite medium model and the isothermal boundary model. In the latter model, the temperature is assumed to remain constant on a plane that is at the elevation of the heater drift floor. In a previous work (Chan et al., 1978), comparison with a fully numerical model in which Newton's Law of Cooling was assumed for the boundary of the drift showed that the true temperature should lie somewhere between the two idealizations mentioned above. For the time scaled experiment, only the infinite medium model has been used since the mid-plane of the heater array is 10 m below the drift floor and the influence of the drift is, therefore, not expected to have a significant effect on temperature. It should be noted that all the thermal models are three-dimensional, although the results are presented in plane sections.

Finite-Element Thermo-Mechanical Models

Thermally induced displacements and stresses were calculated using the finite-element program SAPIV (Bathe et al., 1974). The LBL-LLL version of SAPIV (Sackett, unpublished) combines a bandwidth minimizer and a COMPASS (CDC assembly language) subroutine for dynamic core allocation to allow effective use of small- and large-core memory spaces so that both small and large problems can be handled efficiently. Our temperature program FILINE (based on the method described above) has been interfaced with SAPIV for thermo-mechanical analysis. The program assumes linear thermo-elasticity.

In the present calculations the rock medium is further approximated as a homogeneous, isotropic continuum. This is necessary only because of the lack of data on in situ rock mass properties and conditions. Actually the finite element method is well suited for heterogeneities and the SAPIV program can handle orthotropic, temperature-dependent material properties.

In constructing the finite element models for the full scale experiments two other approximations were introduced:

(1) The system is axially symmetric about the axis of the central heater.

(2) The mid-plane of the heater array is a plane of symmetry.

Two finite-element meshes have been used. The first (hereafter referred to as Mesh 1), consisting of 651 nodes and 607 4-node isoparametric quadrilateral elements, considers the rock medium (except the central heater hole) as an infinite mdeium. In the second mesh (hereafter referred to as Mesh 7) the elements within the heater drift and extensometer drift are removed. Zero normal-displacement boundary conditions were applied to the outer horizontal and vertical boundaries of the model block. Previous work (Chan and Cook, 1979) has confirmed that the fixed boundaries are sufficiently remote from the region where substantial temperature changes occur so that the thermally induced displacements and stresses are practically the same as those obtained using alternative boundary-loading conditions. The alternative analysis for comparison was carried out in the following manner. First a finite element analysis was performed by applying assumed horizontal and vertical virgin stresses to the appropriate outer boundaries of the model with the drifts excavated (i.e., Mesh 7). In addition gravity was applied as a body force to each element. This yielded the mechanical displacements, u_i^{mech}, and stresses, σ_{ij}^{mech},

$$u_i^{mech} = u_i^{vir} + u_i^{exc}, \qquad i = 1,2,3 \tag{5}$$

$$\sigma_{ij}^{mech} = \sigma_{ij}^{vir} + \sigma_{ij}^{exc}, \qquad i,j = 1,2,3 \tag{6}$$

where

u_i^{vir} = displacement (spurious) in the rock continuum caused by applying the virgin stresses as boundary loads and gravity,

u_i^{exc} = displacement induced by excavations,

σ_{ij}^{vir} = stress in the rock continuum caused by applying the virgin stresses as boundary loads and gravity,

σ_{ij}^{exc} = stress induced by excavations.

Next a second run was made with thermal loading added. The total displacement, u_i^{tot}, and a total stress, σ_{ij}^{tot}, would be

$$u_i^{tot} = u_i^{vir} + u_i^{exc} + u_i^{th} \tag{7}$$

$$\sigma_{ij}^{tot} = \sigma_{ij}^{vir} + \sigma_{ij}^{exc} + \sigma_{ij}^{th} . \tag{8}$$

Hence, the thermally induced displacements and stresses are obtained by taking the differences

$$u_i^{th} = u_i^{tot} - u_i^{mech} \tag{9}$$

$$\sigma_{ij}^{th} = \sigma_{ij}^{tot} - \sigma_{ij}^{mech} . \tag{10}$$

The results were found to be in close agreement with those obtained using zero normal-displacement boundary conditions.

In the geological environment of the Hanford NSTF, the reasonableness of the zero vertical-displacement boundary condition for the top boundary requires further confirmation since the experiment horizon is only about 50 m below the surface. A proper analysis can be undertaken with the surface of the earth as a free boundary, but it also requires measured virgin state-of-stress as input. The frequently used relation

$$\sigma_h = \frac{\nu}{1-\nu} \sigma_v$$

where

σ_h = horizontal virgin stress,

σ_v = vertical virgin stress,

ν = Poisson's ratio,

may not be valid since it applies only to a uniaxial strain condition which is not likely to hold at the NSTF site because of the presence of the cliff and slope.

Results and Discussions

Temperatures have been calculated for the full scale experiment for all six power schedules described in the Physical Systems to be Modeled Section and for the infinite medium model and the isothermal boundary model, which are discussed in the Closed-Form Integral Solution for Thermal Analysis Sub-section. Thermally induced displacements and stresses have been calculated only for power schedules 1a and 2a, which give the highest temperatures and, hence, the highest thermal stresses in each of the two groups.

For the time scaled experiment temperatures were calculated using only one power schedule (Figure 4) and one model, the infinite medium model.

Detailed results, which would make this report too voluminous, but which are, nonetheless, necessary for the design of the experiments, are given elsewhere (Chan and Remer, 1978a). Only selected results are highlighted here.

Full Scale Experiments

Temperatures

Figures 5a through 5c and 6a through 6c show the temperature rise in ^{o}C at various radial distances along the mid-plane as a function of time in days of the experiment. Only three power schedules, 1a (5 kW central heater for the first two years), 2a (2 kW central heater for the first two years), and 2c (1 kW central heater for the first two years) have been included.

Due to the low thermal conductivity of Pomona basalt (approximately half that of Stripa granite), exceedingly high temperatures will be reached. In the present calculations the thermal properties at 200^{o}C have been used (values at higher temperatures are not available). Since thermal conductivity of rocks (actually, solids in general) decreases with temperature, even higher temperatures will be predicted if this dependence is taken into account.

Immediately after each power turn-on or power step-up event, the temperature increases very rapidly within the radius of the peripheral heater array

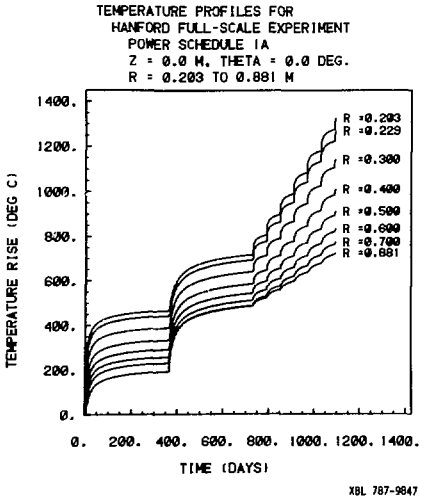

(a)

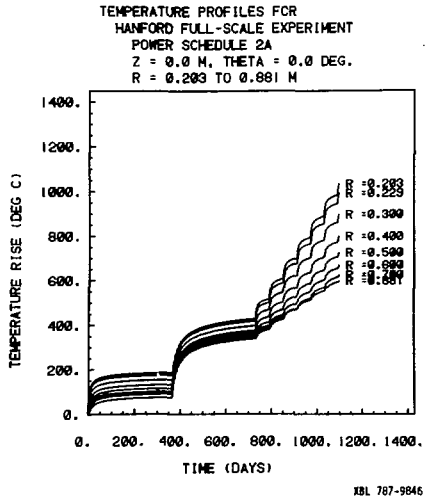

(b)

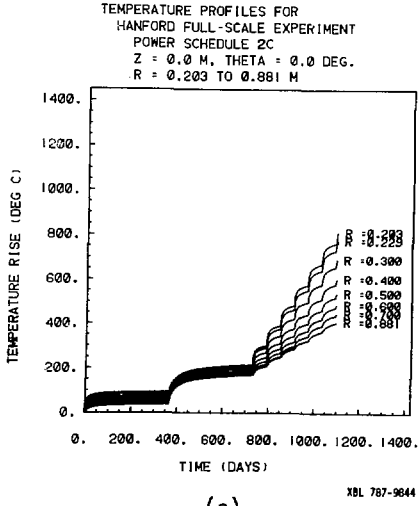

(c)

Figure 5. Temperature Profiles for Hanford Full-Scale Experiment, R = 0.203 to 0.881.

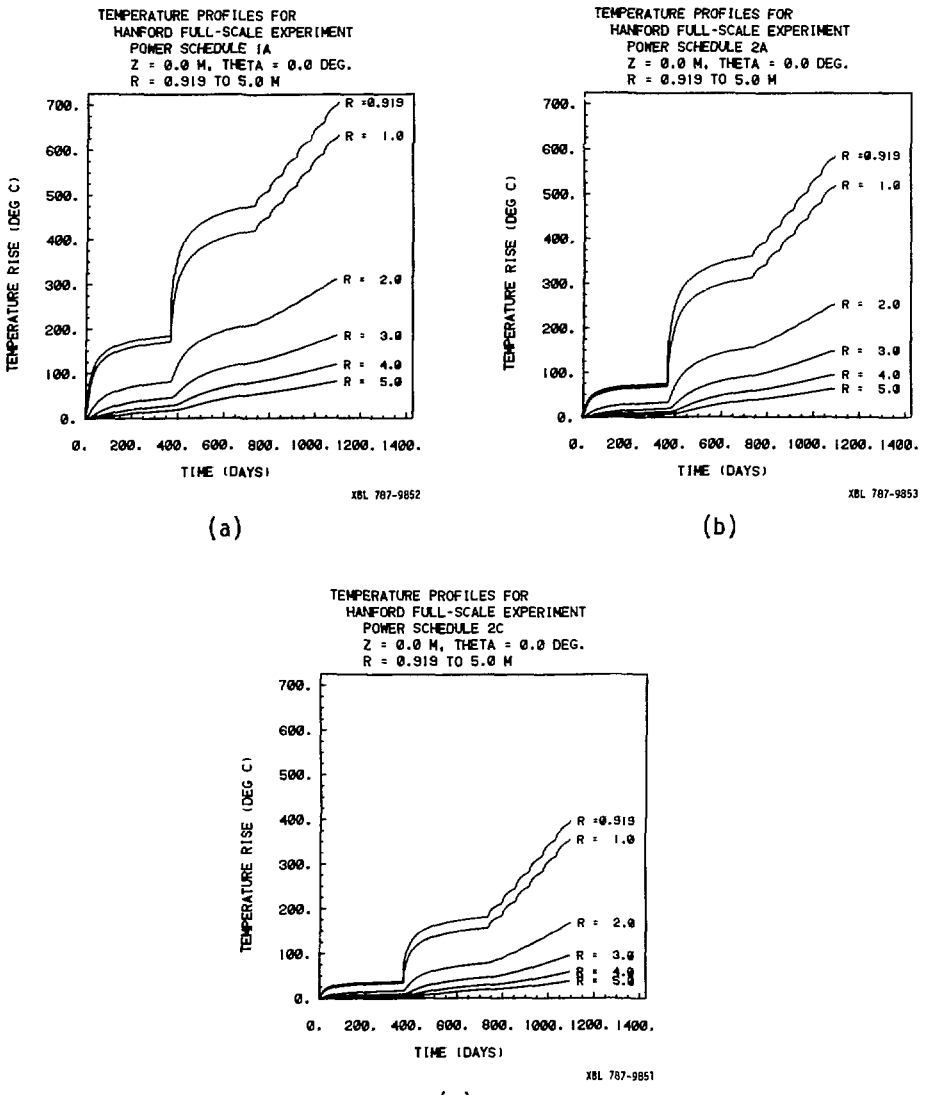

Figure 6. Temperature Profiles for Hanford Full-Scale Experiment, R = 0.0919 to 5.0.

for 20 to 30 days. Thereafter, the rise becomes more gradual so that after 50 to 60 days the temperature changes so slowly that the heater-rock system can be said to be approaching a quasi-steady state. This shows that the 60 day duration between successive power steps is sufficient time for observation of the thermal effects due to a particular power step. Within a radius of 1 m from the central heater, distinct steps can be recognized on the temperature curves corresponding to successive power steps (Figure 5a through 5c). Beyond 1 m the pulse nature of the power increase is attenuated by distance and the temperature rise follows smooth curves (Figure 6a through 6c). Another important point to note is that the ring of 1 kW peripheral heaters increases the temperature within its circumference by 250°C. This represents a very extreme case of the ambient temperature field due to other waste canisters.

Table 3 gives the temperature rise at the end of the first, second, and third years of the full scale experiment for selected values of r. Maximum increases in rock temperatures at the end of the first, second, and third years have been predicted to be 440°C, 690°C, and 1270°C for the highest power considered (Schedule 1a) and 85°C, 210°C, and 775°C for the lowest power considered (Schedule 2c).

Since some of the predicted temperatures exceed the temperature ratings of the extensometers and USBM- and IRAD-guages, as well as exceed the highest temperatures at which the heaters have been tested in mock-up experiments, failure is likely to occur during the full scale experiments. Table 4 summarizes the temperature ratings of the heaters and instruments, other significant temperatures, and the times at which these temperatures will be attained. Clearly some of the temperatures predicted for the later stages of the full scale experiments are hypothetical. A number of drastic events such as heater failure, thermal run-away resulting from borehole decrepitation, or rock melting would have happened, invalidating the present calculations.

Examples of isotherm contours in longitudinal sections are given in Figure 7a through 7e. Comparison of Figure 7a and 7b shows that the effect of the assumed boundary condition is already manifested by the asymmetry of the 5°C isotherm for the isothermal boundary model. However, the maximum rock temperatures reached at the edge of the central heater hole differ very little between the two models. It is interesting to note that within a 0.5 m radius of the central heater, the temperature is practically independent of z over the length of the heater. On the other hand, a vertical thermal gradient always exists above and below the heater.

TABLE 3. Calculated temperature rise (^{o}C) at the end of the first, second, and third years of the full scale experiment.

		Power Schedules					
Time	Value of r(m)	1a	1b	1c	2a	2b	2c
First Year	0.229	440	430	220	175	170	85
	0.5	290	280	135	125	120	65
	1.0	170	163	88	70	65	35
	2.0	80	75	40	30	25	15
	5.0	25	12	7	5	5	2
Second Year	0.229	690	560	345	420	300	210
	0.5	535	420	265	360	235	180
	1.0	420	300	215	310	190	160
	2.0	210	150	100	155	90	75
	5.0	50	35	25	35	22	15
Third Year	0.229	1270	1140	915	1000	860	775
	0.5	885	755	615	695	575	405
	1.0	630	510	405	520	38[c]	350
	2.0	312	240	190	250	185	165
	5.0	80	60	45	67	40	35

TABLE 4. Significant temperature values and predicted times at which temperature is attained for the infinite medium model, power schedules 1a, 1b, 1c, 2a, 2b, 2c.

Temperature (Centigrade)	Significance	Value of r (meters)	Time (days) temperature value is reached at designated value of r					
			1a	1b	1c	2a	2b	2c
100°	Boiling point of water	0.229	1.2	4	4	7	181	371
200° - 250°	Estimated temperature ratings of instruments++	0.5	60-90	190 -215	395 -415	380 -400	420 -735	740 -800
		1.0	360 -375	375 -415	560 -819	390 -435	735 -835	805 -900
		2.0	640 -890	945 -*	1095 -*	900 -1075	*	*
500° - 600°	Estimated temperature rating of heater assembly	.229	385 -420	395 -740	815 -910	760 -860	860 -920	910 -980
1050°	Incipient melting point of basalt+++	.229	980	1085	*	*	*	*

* Temperature is not reached within the three year test period.

++ This includes extensometers, IRAD and USBM gauges.

+++ Ekren, et al., 1974. See also Presnall, et al., 1972.

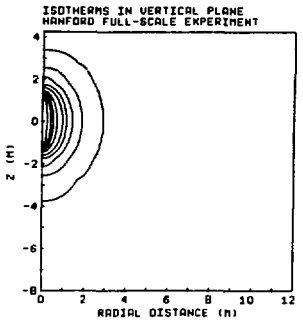

XBL 787-9499

(a)

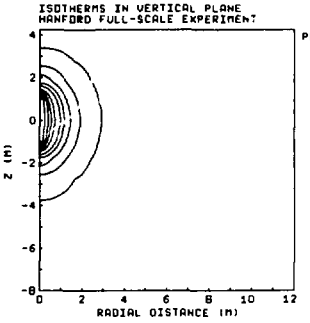

XBL 787-9473

(b)

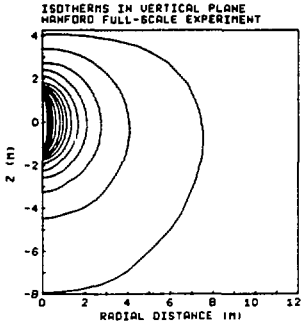

XBL 787-9471

(c)

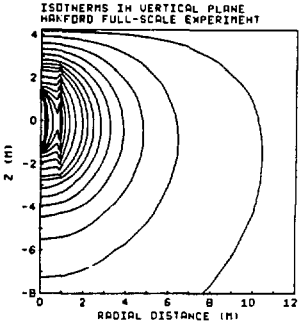

XBL 787-9472

(d)

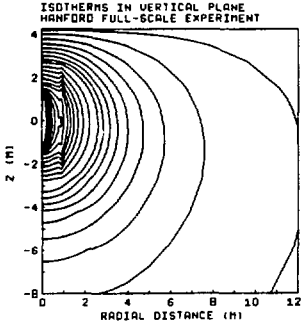

XBL 787-9465

(e)

Figure 7. Isotherms in Vertical Plane, Hanford Full-Scale Experiment.

Because of the low thermal diffusivity of Pomona basalt, the high temperature zone is very localized. For example, the 100°C incremental isotherm has moved radially outward from the 5 kW central heater by only 2 m during the first year (Figure 7b) and by an additional 1.5 m during the second year (Figure 7c). For the 2 kW central heater, the migration is even slower, approximately 0.5 m during the first year and another 1.25 m during the second year.

Displacements

Sample results for thermally induced displacements are illustrated for Power Schedule 1a in Figure 8a through 8d (Mesh 1, drifts not modeled) and Figure 9a through 9b (Mesh 7, drifts modeled) for radial displacement (u_r) vs. radial distrance (r) and in Figure 10a through 10b for deformation of the periphery of the heater drift. Tables 5, 6, and 7 summarize the maximum predicted radial-displacements (u_r), the maximum vertical displacement (u_z) at various radial distances, and maximum vertical displacements immediately beneath the floor of the heater drift at different times.

The peak of the u_r curve moves away from the central heater as time progresses (Figure 8a through 8d). Maximum radial displacements at the end of the first, second, and third years were found to be 0.8 mm, 2 mm, and 3 mm for Power Schedule 1a and 0.35 mm, 1.5 mm, and 2.5 mm for Power Schedule 2a (See Table 1b and Figure 2 for the power schedules). The presence of the heater and extensometer drift has little effect on the maximum values of u_r (Table 5) but has a remarkable effect on the radial distribution of u_r at longer times, c.f. Figure 8c, 8d and 9a, 9b. Notice also that the radius of the central heater hole is reduced as the rock heats up. This is a result of confinement.

Maximum vertical displacements are about twice as large as the maximum radial displacements. This can be attributed to the elongated shape of the heated zone and the proximity of the heater drift to the heaters. The significance of the presence of the heater drift can be seen in Figure 10a and 10b where the symbols designated "Mesh 1" represent the deformation of an imaginary boundary in an infinite rock medium and those symbols designated "Mesh 7" represent the deformation of the periphery of the heater drift, which is tilted by the thermal loading. It should be possible to measure the deformation of the drift periphery with convergence meters. Such information would be useful in repository design.

Stresses

Examples of the normal components of the thermal stress as a function of radial distance along the heater mid-plane are shown in Figure 11a through 11e at different times for Power Schedule 1a. Initially, over a short range of

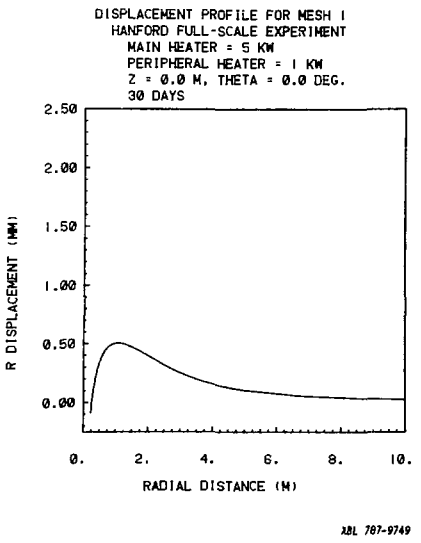

(a)

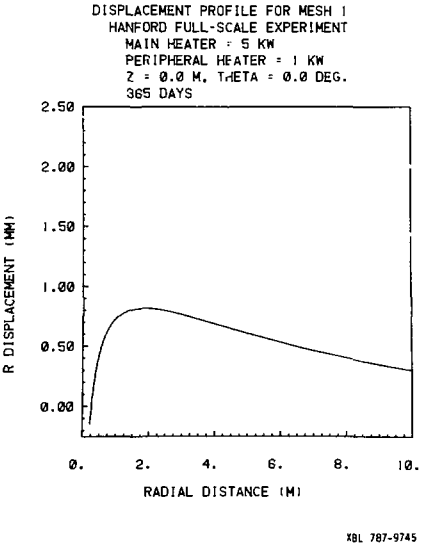

(b)

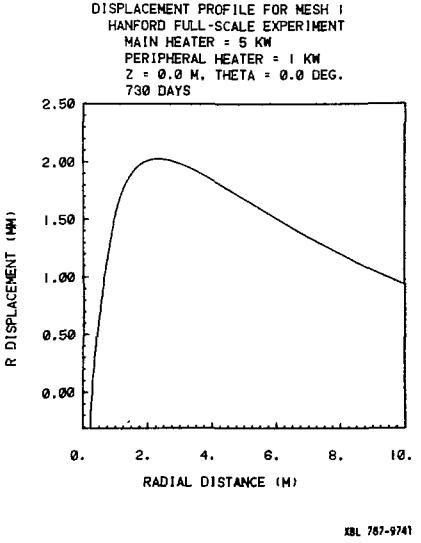

(c)

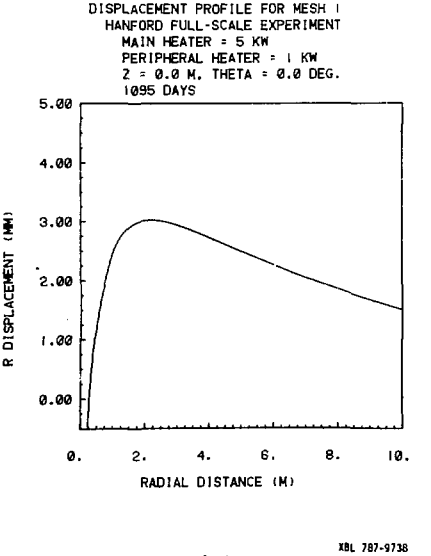

(d)

Figure 8. Displacement Profile for Mesh 1, Hanford Full-Scale Experiment.

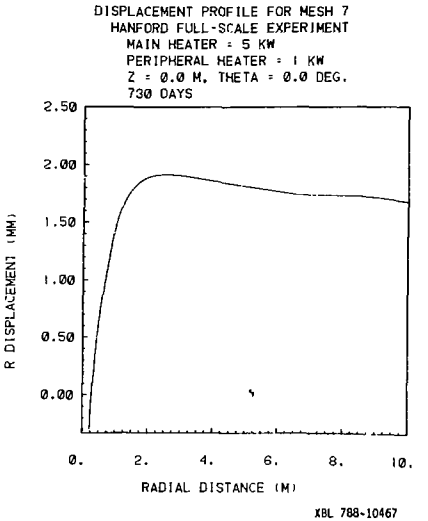

(a)

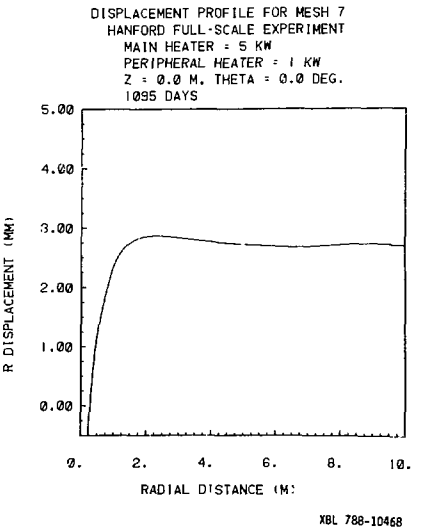

(b)

Figure 9. Displacement Profile for Mesh 7, Hanford Full-Scale Experiment.

TABLE 5. Maximum predicted radial displacement in the midplane.

		Power Schedule 1a		Power Schedule 2a	
	Days	max U_r (mm)	Value of r(m) at which Max U_r occurs	max U_r (mm)	Value of r(m) at which Max U_r occurs
Mesh 1	7	.27	.75	.11	.75
	30	.50	1.2	.20	1.1
	90	.66	1.5	.27	1.4
	180	.75	1.7	.30	1.55
	365	.82	1.9	.35	1.90
	371	1.04	1.5	.55	1.40
	390	1.35	1.5	.85	1.6
	450	1.68	2.0	1.15	1.9
	730	2.04	2.3	1.50	2.5
	760	2.10	2.35	1.58	2.3
	790	2.15	2.4	1.64	2.4
	1095	3.00	2.2	2.48	2.2
Mesh 7	730	1.91	2.5	1.41	2.60
	1095	2.90	2.25	2.35	2.30

TABLE 6. Maximum predicted vertical displacements and the value of Z at which the maximum displacements occur. Mesh 1 and Mesh 7 at 730 and 1095 days. R = 0.45, 1.875, 10.5 m.+

Power Schedule			Mesh 1 value of r (m) 0.45	Mesh 1 value of r (m) 1.875	Mesh 1 value of r (m) 10.5	Mesh 7 value of r (m) 0.45	Mesh 7 value of r (m) 1.875	Mesh 7 value of r (m) 10.5
730 days	1a	max u_z (mm)	2.10	1.68	0.38	3.90	3.00	0.38
		z (m)	3.85	3.70	7.50	++	++	6.50
	2a	max u_z (mm)	1.55	1.24	0.24	2.90	2.20	0.26
		z (m)	3.85	3.55	7.50	++	++	6.50
	combined	max u_z (mm)	--	--	0.62	--	--	0.64
		z (m)	--	--	7.50	--	--	6.50
1095 days	1a	max u_z (mm)	3.10	2.48	0.63	5.80	4.30	0.62
		z (m)	2.65	3.60	8.00	++	++	7.50
	2a	max u_z (mm)	2.55	2.02	0.49	4.70	3.60	0.48
		z (m)	2.65	3.50	8.00	++	++	7.50
	combined	max u_z (mm)	--	--	1.10	--	--	1.10
		z (m)	--	--	8.00	--	--	7.50

+ The value of r is the distance from the centerline of the central heater of the respective experiment. The value of r = 10.5 m is the only point at which the vertical displacements have been combined (assuming that the two full-scale experiments are separated by 21 m).

++ The maximum displacement occurs at the floor of the heater drift, z = 4.25 m.

TABLE 7. Maximum predicted vertical displacement 0.375 meters below the floor of the heater drift. Mesh 1 and Mesh 7.

Maximum Value of U_z	Power Schedule 1a		Power Schedule 2a	
	Mesh 1	Mesh 7	Mesh 1	Mesh 7
730 Days	2.0	4.2	1.5	3.2
1095 Days	2.8	6.2	2.4	5.0

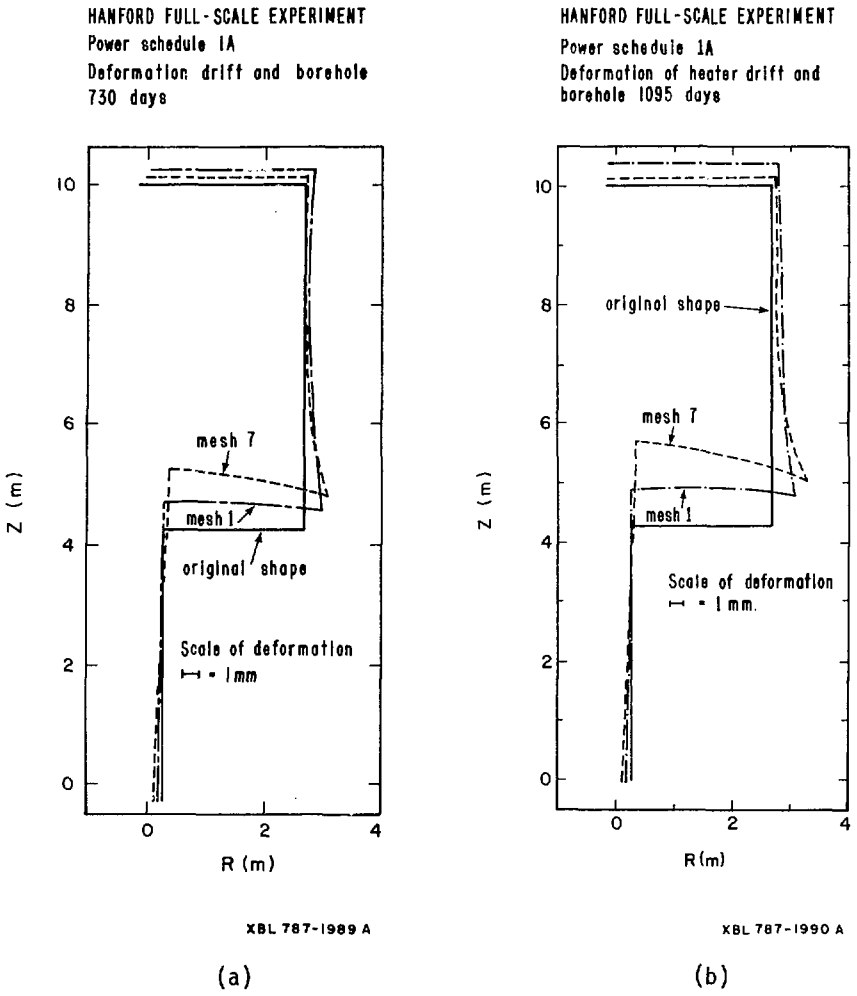

Figure 10. Hanford Full-Scale Experiment--Deformation of Drift and Borehole.

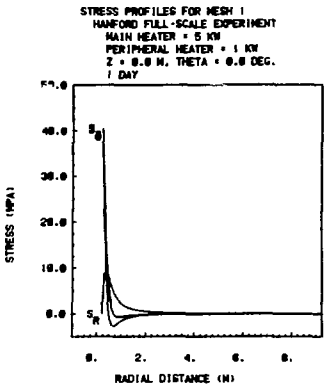

(a)

XBL 788-9862

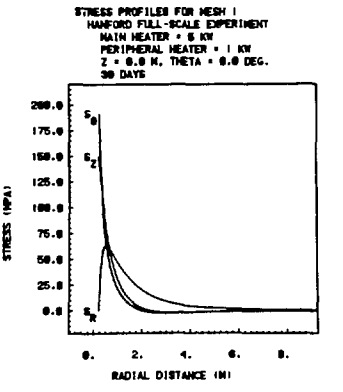

(b)

XBL 787-9736

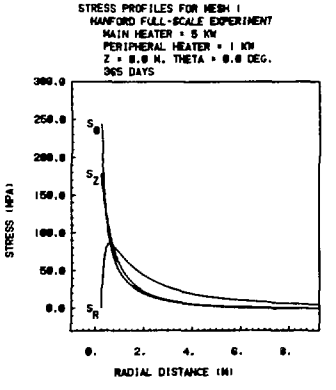

(c)

XBL 787-9697

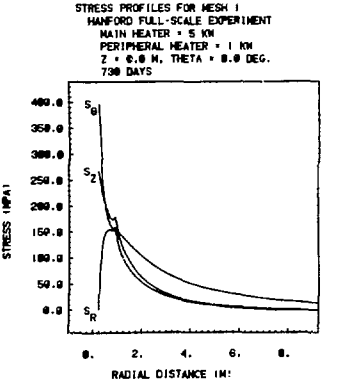

(d)

XBL 787-9701

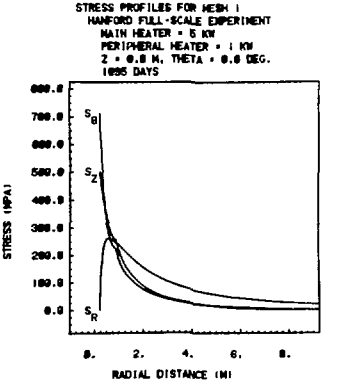

(e)

XBL 787-9704

Figure 11. Stress Profiles for Mesh 1, Hanford Full-Scale Experiment.

distance from the central heater, both the axial stress (σ_z) and tangential stress (σ_θ) are tensile with a maximum magnitude of 1 MPa. This tensile portion rapidly spreads out and diminishes in magnitude as time progresses. At the edge of the hole, both σ_z and σ_θ are compressive and reach high values even at relatively short times. For example, 30 days after turn-on of the 5 kW central heater (Figure 11b) σ_z (150 MPa) and σ_θ (191 MPa) already fall well within the range of values for the uniaxial compressive strength of Pomona basalt (75-378 MPa as measured by Duvall et al. (1978) in small intact specimens). Consequently, thermal decrepitation may occur early in the experiment. However, if the rock mass has uniaxial compressive strength equal to the average value (284 MPa) given by Duvall et al. (1978), then failure will occur only after the peripheral heaters are turned on. The peripheral heaters enhance the general level of thermally induced stresses as well as introducing a subsidary peak in the σ_z vs. r and σ_θ vs. r curves.

Tables 8 and 9 summarize the maximum compressive stresses (in the heater mid-plane) and the maximum tensile stresses (immediately beneath the floor of the heater drift) predicted for Power Schedules 1a and 2a. Those tensile stresses, σ_θ in particular, are extremely high, exceeding the mean tensile strength of intact Pomona basalt given in the reference quoted above. According to a recent hydrofracture measurement by Haimson (1978), the horizontal components of the virgin state of stress in the NSTF horizon are approximately 0.7 MPa and 7-14 MPa in the directions normal and parallel to the length of the ridge. The net tensile stress will thus exceed the tensile strength some time during the experiment in both cases given in Table 9, and cracking of the drift floor is likely to occur if the rock is behaving as a linear elastic continuum.

In addition, the very small horizontal in situ stress in one direction casts some doubt on the validity of an axisymmetric model with fixed displacement-boundary condition. A first step in checking the validity of the displacement boundary condition would be to repeat the stress calculation by applying the minimum in situ horizontal stress to the outer boundary of the axisymmetric model and compare the results with the fixed boundary model. If the results agree, then the axisymmetric model with fixed displacement-boundary condition can still be applied. The total resultant stress can be obtained by superposition if the rock is assumed to be a linear elastic continuum.

In the present preliminary calculations, the rock mass has been treated as a continuum as a first approximation. In reality numerous discontinuities

TABLE 8. Maximum predicted compressive stresses in the heater midplane, Mesh 1.

Stress (MPa)/ Power Schedule

Days	max σ_r +		max σ_θ ++		max σ_z ++	
	1a	2a	1a	2a	1a	2a
1	9.2	3.7*	40.3	16.1	40.6	16.2
7	38.0	15.2	129.3	51.7	112.4	45.0
30	63.0	25.2	191.9	76.7	150.1	60.0
90	75.7	30.2	222.5	89.0	166.7	66.7
180	81.0	32.4	235.4	94.1	173.5	69.4
365	85.1	34.0	244.8	97.9	178.4	71.4
371	94.9	43.9	264.2 93.4	117.2 61.4	189.7 109.4	82.6 71.8
390	115.7	66.1	312.2 114.3	164.9 82.1	221.4 134.7	114.2 96.8
450	136.0	87.3	358.1 137.6	209.9 104.9	247.6 158.6	139.9 120.4
730	154.4	105.2	397.4 159.0	246.6 125.0	268.4 179.2	159.4 139.6
760	166.8	115.7	437.4 165.1	286.4 130.9	299.3 187.3	190.1 147.5
790	169.4	118.3	443.1 168.0	291.9 133.7	302.3 190.1	193.1 150.3
1095	261.8	208.2	714.3 -	561.7 -	502.8 -	392.9 -

*Maximum value occurs between 0.4 and 0.9 m.

**Maximum value occurs at edge of heater hole, r=0.229m; where two values are given, second value is local maximum near $r = 0.9$m.

TABLE 9. Maximum predicted stresses (σ_r,σ_θ) 0.375 meters below the floor of the heater drift. Mesh 7, power schedules 1a and 2a.

		Maximum Tensile[+]		Maximum Compressive	
	Days	1a	2a	1a	2a
σ_θ (MPa)	730	34	27	12	8
	1095	48	42	18	14
σ_r (MPa)	730	16	15	42	32
	1095	23	20	62	50

[+]These values are the maximum of the absolute value of the tensile stress.

of various sizes and spacings exist in the rock mass (Goodman, 1976). The closely spaced discontinuitites can be treated by an equivalent medium approach in which the rock mass is modeled as an anisotropic continuum with reduced elastic moduli. The larger discontinuities have to be modeled individually (Goodman et al., 1968; Noorishad et al., 1971; Gale et al., 1974; Ayatollahi, 1978; Ayatollahi and Chan, work in progress). In view of the lower elastic moduli and possibly lower thermal-expansion coefficient expected in a fractured rock mass, the thermal stress and displacement would be lower than those predicted here using a continuum model. This has been found to be the case during the Stripa experiments (Cook and Hood, 1978). In particular, tensile stresses may or may not be transmitted across discontinuities. On the other hand, the in situ compressive and tensile strengths may also be substantially below the intact rock values, and therefore both compressive and tensile failure may still occur with consequent lowering of thermal conductivity and enhancement of permeability. It is necessary to measure the elastic moduli and the joint stiffness and thermal expansion coefficient along with their temperature and time dependence in situ and/or in large blocks of rock containing discontinuities in order to provide realistic input parameters for proper nonlinear numerical modeling.

Interference between Two Full-Scale Experiments

Interference between two full-scale experiments at 21 m separation operated under Power Schedules 1a and 2a is illustrated in Figure 12 for temperature rise, Figure 13 and Table 10 for radial displacement, and Figure 14 for radial stress. It is seen that the two experiments are practically thermally independent. After 730 days the temperature field is still very localized so that the combined temperature rise midway between the two experiments is less than 2% of the maximum rock temperature due to the higher power experiment alone. With regard to the thermally induced displacement, however, the two experiments interact very strongly. For example, at a distance of 12 m from the 5 kW heater along the line joining the centers of the two central heaters, the radial displacements (u_r) canceled, whereas the value for each individual experiment would be close to 40% of the individual maximum u_r. Even near each central heater, the effect of the other experiment is not negligible (Table 10). Similarly the two experiments also affect each other significantly in vertical displacements. Interference of the radial stresses due to the two experiments is moderately serious (Figure 14).

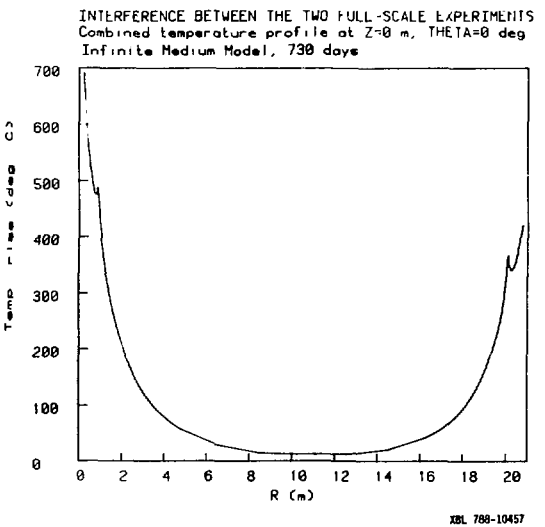

Figure 12. Interference Between the Two Full-Scale Experiments -- Temperature Profiles.

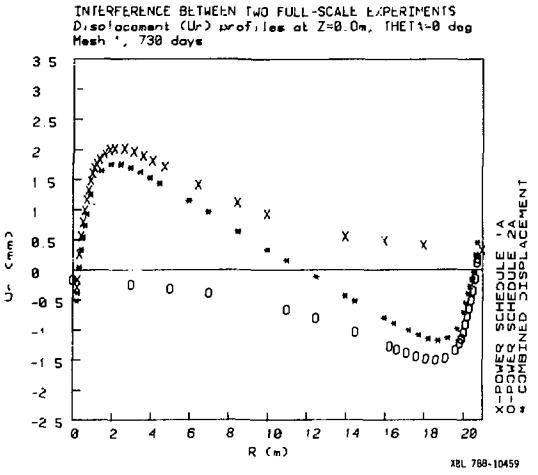

Figure 13. *Interference Between the Two* Full-Scale Experiments -- Displacement Profiles.

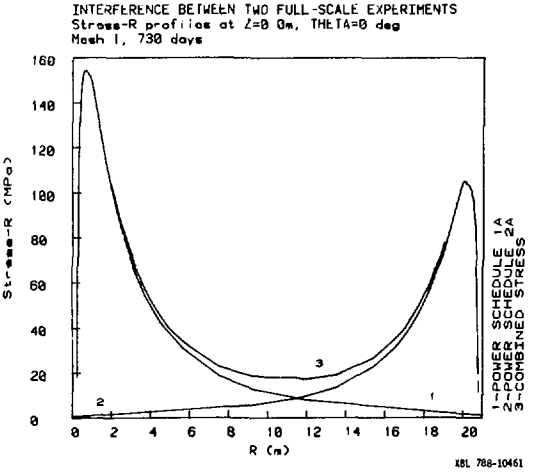

Figure 14. Interference Between the Two Full-Scale Experiments -- Stress Profiles.

TABLE 10. Predicted combined radial displacements in heater midplane of the two full-scale experiments, Mesh 1.
(a) 730 days (r = 2.5, 5.0, 10.5, 12.0, 16.0, 18.5+)
(b) 1095 days (r = 2.0, 5.0, 10.5, 11.75, 16.0, 19.0+).

	730 Days					
u_r (mm)	Value of r (m) 2.5	5.0	10.5	12.0	16.0	18.5
Power Schedule 1a	2.00	1.65	0.85	0.75	0.45	0.30
Power Schedule 2a	-0.25	-0.35	-0.60	-0.75	-1.25	-1.50
Combined	1.75	1.30	0.25	0.00	-0.80	-1.20
Fractional Change*	0.125	0.212	0.706	1.00	0.36	0.20

	1095 Days					
u_r (mm)	Value of r (m) 2.0	5.0	10.5	11.75	16.0	19.0
Power Schedule 1a	3.00	2.50	1.50	1.25	0.80	0.50
Power Schedule 2a	-0.50	-0.75	-1.10	-1.25	-2.00	-2.50
Combined	2.50	1.75	0.40	0.00	-1.20	-2.00
Fractional Change*	0.167	0.30	0.733	1.00	0.40	0.20

+Value of r is the distance from the full scale experiment with power schedule 1a to that with power schedule 2a.

The direction of positive displacement is away from the full scale experiment with power schedule 1a.

*Fractional Change = $\left| \frac{u_r(\text{nearest experiment}) - u_r(\text{combined})}{u_r(\text{nearest experiment})} \right|$

In the interpretation of the field data, comparison should be made with the superposed predicted displacements and stresses, otherwise the experimental results may be misunderstood as being due to anisotropy of the rock mass.

Time Scaled Experiment

Example contour plots of incremental isotherms are shown in Figure 15a through 15d at different stages of the time scaled experiment. The effect of spacing is apparent. Two heaters at 3 m spacing start interacting earlier than those at 7 m spacing and interact at a high temperature throughout the experiment. The secondary heaters start interacting with the primary heaters one week after they are turned on (Figure 15c). Toward the end of the experiment, moderately high isotherms for all heaters have coalesced (Figure 15d).

The wall of the heater hole reaches 300°C in the first 10 days and never exceeds 400°C. Switching on the secondary heaters increases the temperatures near a primary heater by about 30°C. At a radial distance of 0.5 m from any heater, the maximum temperature increase at any time is less than 200°C. Consequently instrument failure is unlikely outside the 0.5 m radius.

As a rough check of the accuracy of scaling, note that at r = 3.2 m, z = 0, time = 310 days (Figure 6a). The temperature rise for a 3.6 kW full scale heater (to which each time scaled heater corresponds) is approximately 32°C ($45 \times 3.6 / 5 \approx 32$). From Figure 15a we see that this is also the temperature rise at 1 m radius from a 1.125-kW scaled heater ($1.125 \times 3.2 = 3.6$) at a time of 30 days.

In the calculations presented above for the time scaled heater experiment, the heaters were assumed to have constant power. If a decaying power is used to simulate heat generation from radioactive waste, the temperature will reach a peak value and then start declining. This has been found to be the case in the calculated temperatures for a similar time scaled experiment in Stripa (Chan and Remer, 1978b). The maximum rock temperature reached at the edge of a heater hole will be about the same, but the maximum temperatures further away from the individual heaters will be lower.

Recommendations

One of the full scale experiments may be run with the central heater at 5 kW and the peripheral heaters at 1 kW as a "test to failure." The period between energizing the central heater and peripheral heaters may be shortened to about 6 months. Passive, microseismic detection techniques would be very useful in determining both the time of occurrence and location of thermally induced cracking.

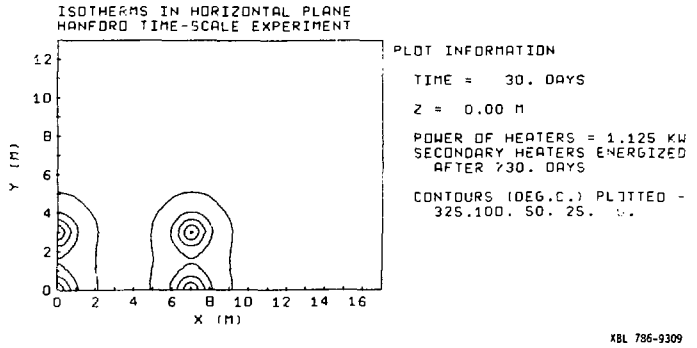

(a)

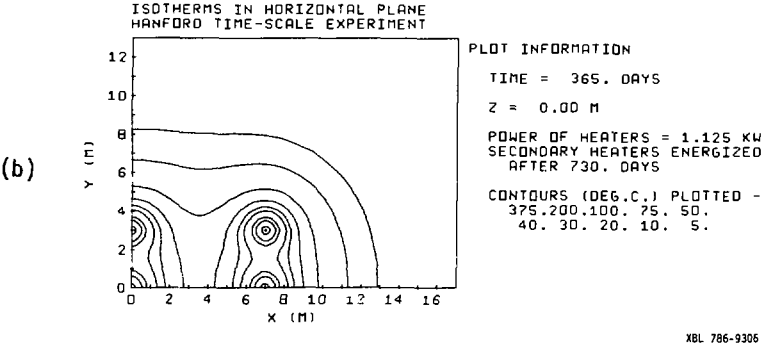

(b)

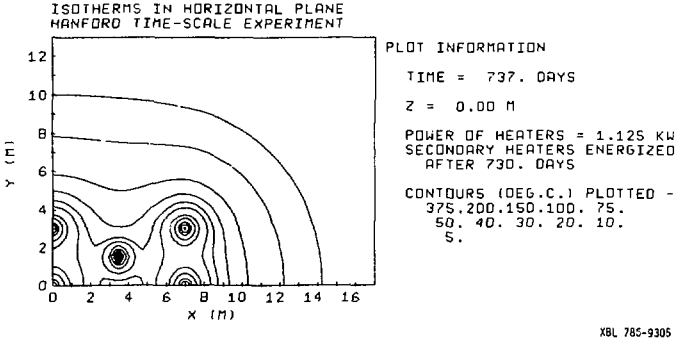

(c)

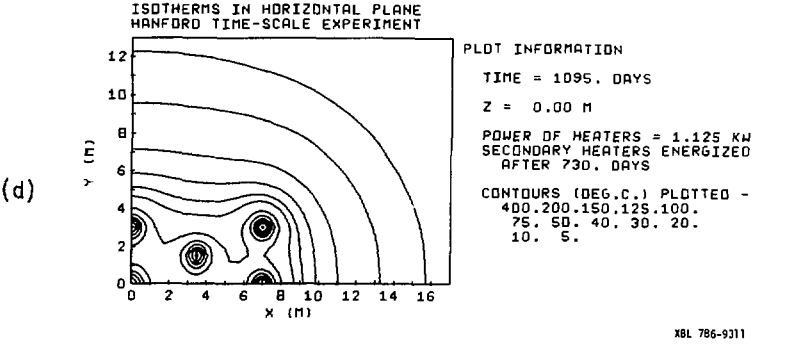

(d)

Figure 15. Isotherms in Horizontal Plane -- Hanford Time-Scale Experiment.

The other full scale experiment should be run with the central heater at 1 to 2 kW and the peripheral heaters at 0.5 kW. In this way sufficient data on the thermo-mechanical response of the Pomona flow can be collected before the instruments fail.

The convergence between the floor and roof of the full scaled heater drift can be measured with extensometers. This may facilitate the determination of the amount of floor heave prior to the occurrence of tension fractures on the floor. The information would be useful for repository design as well as for monitoring during the operating phase. In a repository it may be necessary to place the waste canisters in deeper drillholes to mitigate the effects of tension fractures.

In view of the low thermal conductivity of Pomona basalt, unless the results of the heater experiments indicate otherwise, it would be prudent to limit the initial power of any spent fuel canister placed underground to 0.4 kW/m (corresponding to a 1-kW full scale heater of 2.5 m length) to ensure that the temperatures of the fuel cladding does not exceed 200°C.

The interference between the two full-scale experiments should be taken into account in the analysis of the displacement and stress data.

A few extensometers should be placed near the midpoint of the center-to-center line of the two full-scale heaters to assess the thermo-mechanical interaction.

Further temperature calculations whould be carried out for the time-scaled heater experiments using the finite-line source model adopted in this report with decaying sources.

Detailed thermo-mechanical modeling taking into account the discontinuities in the rock should be carried out. To provide meaningful inputs for such models, the thermal and mechanical properties and their temperature and time dependence should be measured in situ as well as in large rock samples containing fractures. Furthermore the fracture pattern of the site has to be mapped out in detail.

Since the temperature fields in all these heating experiments are localized, it is necessary to carry out larger scale heating experiments to investigate thermo-mechanical response on an excavation and repository scale.

IV. HEATER AND ROCK INSTRUMENTATION LAYOUT

A. DuBois

A proposed arrangement for the 31 heater and 216 rock instrumentation boreholes specified for the three NSTF heater experiments was prepared. The borehole locations, dimensions, and specifications were presented in tabular form (LBL Engineering Note M5227) with supporting drawings (LBL No. 19G0016, 10G0026, 19G0036, 19G0046, 19G0054, and 19G0064) showing the physical relationships between these boreholes and the NSTF drifts in which they were to be installed.

The rock instrumentation that was proposed for mounting in these boreholes was described in a report by Terra Tek, Inc. (LBL subcontract Purchase Order 4099002). This report was issued in a revised form during August 1978 with a subsequent addendum dated August 29, 1978.

V. HEATERS AND CONTROLS

G. Binnall and A. DuBois

Introduction

Several electrical heaters are to be installed within the NSTF to simulate the discrete heat loads to be expected from canisters of nuclear waste. These heaters are scheduled to run for a period of approximately two years plus a possible overload for one year. The heater designs have been adapted from similar heaters designed by Lawrence Berkeley Laboratory for Stripa. Recent changes being considered for the Rockwell test plan may require changes in the designs described below.

In reengineering the Stripa heaters for the Hanford NSTF installation, 33 new mechanical drawings and three heating element specifications have been generated. The remaining 38 mechanical details have been adapted from the earlier Stripa designs. Of these drawings, 6 have been marked to show suggested changes. LBL drawing trees which show the identity and relationship of these drawings are: 19B4143, 19B4093, 19B3993, and 19B3933.

The electrical heaters are of three types: (1) Full scale (2) Peripheral and (3) Time scale. Descriptions of the heaters and their auxiliary equipment are given below.

The full scaled heaters are designed to duplicate the geometry (12.75-in.-diameter x 8.5-ft-long) of one possible canister and to provide a heat load (5 kW maximum) which might be delivered by such a waste container. Two such heaters will be installed at widely separated locations within the excavation. One heater will operate at high power in a lined borehole. The second unit will operate at a lower power level and may be installed in an unlined borehole. Either or both of these units may operate within the thermal field of eight peripheral heaters.

The peripheral heaters are one-inch-diameter low-power units (1.0 kW) whose heat output simulates the thermal environment which would surround a typical waste container located within a large field of containers. Eight of these peripheral heaters are to be installed in a circular array (3-feet radius) around each full scale heater.

A group of thirteen time scale heaters are to be installed at a third isolated location within the NSTF. These heaters are approximately one-third of the size and power of the full scale heaters. Modeling laws were used to select this scaling factor and the heater spacing so that the installed units

would create a thermo-mechanical response whose time constant would be one-tenth of that for a full scale heater. These time scale heaters are to be arranged in a rectangular array to simulate the heat load and distribution of a large field of waste storage canisters.

The principal elements of each heater installation are:

(1) A vertical borehole in the mine floor for receiving the heater assembly.

(2) A cylindrical enclosure (canister) which houses the electrical heater elements.

(3) The electrical heater elements.

(4) The electrical leads.

(5) An upper tube to support the canister and the leads.

(6) A thermal insulation plug to prevent heat loss up the borehole.

The following are optional features:

(7) A borehole liner.

(8) Temperature monitoring equipment.

(9) A borescope and guide tubes for inspecting the borehole wall.

(10) Dewatering apparatus to remove liquid and steam from the borehole.

Full-Scale Heater

The design criteria for the full scale heaters include:

(1) Simulating a 12.75-in.-diameter x 8.5-ft-long cylindrical canister filled with nuclear waste material buried at the bottom of a 18-in.-diameter x 18-ft-deep borehole in a hard granitic rock formation. Thermal output of the nuclear waste material will not exceed 5 kW.

(2) Providing heat by a 208-volt, 60-Hz power source. Heat to be uniformly distributed along the length of the canister and centered 14 feet below the floor of the drift.

(3) Providing maximum redundancy in case of heater element failure and designing equipment for a test duration of three years minimum.

(4) Designing for a maximum temperature of the wall of the borehole which is approximately 710^{o}C after 2 years at 5 kW.

(5) Providing thermocouples for monitoring the temperature of the canister at its mid-length plus the temperature near the heater element terminals.

(6) Providing means for measuring the temperature of the lower heating element spacer sheet and the bottom of the canister using an optical pyrometer.

(7) Providing thermal insulation to minimize heat loss up the borehole.

(8) Designing for installation in a drift having limited (17 feet) ceiling clearance.

(9) Designing for possible removal from the borehole.

(10) Providing a dry collar surrounding the top of the rock bore to prevent water on the tunnel floor from entering the bore.

(11) Providing a borehole liner for one heater.

(12) Making it possible to view the heated portion of the borehole with a borescope.

(13) Providing equipment to remove water and steam from the annular space between the cylindrical tank and the borehole and to measure both the water and the steam flow rate simultaneously.

(14) Providing a portable thermocouple for monitoring the temperature of the borewall, the liner, and the canister.

The installation of a full scale heater is shown in Figure 16. The assembly is constructed in a modular fashion (see Figure 17) to facilitate its installation with limited overhead clearance and to provide subunits conveniently sized for shipping to a remote location.

Figure 16 shows the heater installation in both a lined and an unlined borehole. The liner has not yet been designed; however, certain assumptions regarding the liner diameter and length are implicit in the layout of the heater installation. The outer diameter of the liner is assumed to 15.5 in. with a 0.5-in.-thick wall and the length is assumed to be approximately the same as the canister length.

The cylindrical heater enclosure (see Figure 18) simulates a waste canister. It is an AISI 304 stainless-steel pipe--nominal 12 in., schedule 10. Actual outside diameter is 12.75 in., wall thickness is 0.18 in., and length is 8.5 ft. It is closed at the bottom with a welded plate (with a small drain hole) and at the top by a demountable flange which is part of the heater element support.

Computer modeling provided a prediction of the time vs. temperature history for a basalt borehole subjected to a 5-kW continuous heat load for two years. The 710°C maximum borehole temperature predicted by this model was used as a boundary condition for estimating the maximum canister-wall temperature. At this temperature, the dominant heat transfer mode is radiant. A maximum canister temperature of 724°C was predicted based on an emissivity of 0.9 for the borehole, 0.7 for the oxidized stainless steel tube, and a geometry factor of 0.66 for the concentric tube geometry.

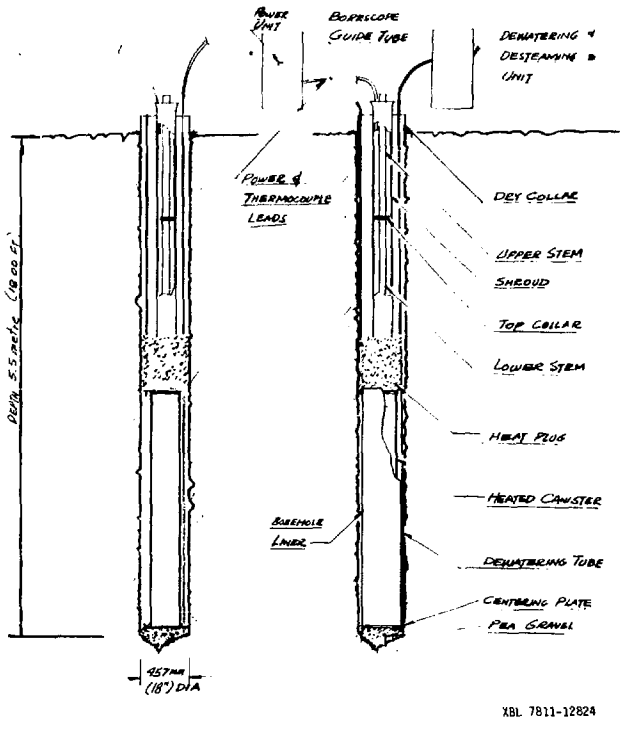

Figure 16. Full-Scale Heater Installation in a) Unlined Borehole, b) Lined Borehole.

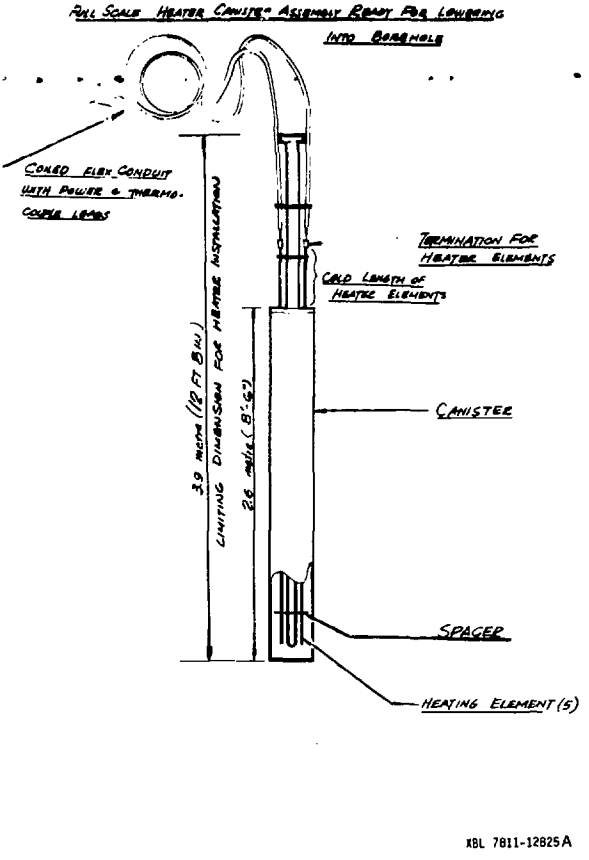

Figure 17. Full Scale Canister Assembly Ready for Lowering Into a Borehole.

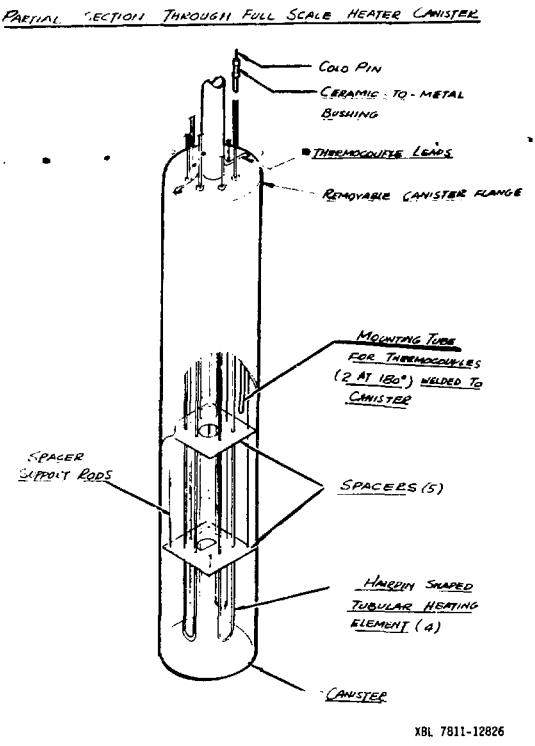

Figure 18. Partial Section Through a Full-Scale Heater Canister.

Two 0.63-in.-diameter thermocouple mounting tubes are provided along the inside wall of the canister. These tubes are parallel to the centerline of the canister and are welded to it. Prior to lowering the canister into the borehole, one type-K (Chromel-Alumel) thermocouple is to be inserted into each tube. The T.C. junction is to be located at the canister mid-plane. Each thermocouple is mineral insulated inside an Inconel sheath of 1.6-mm (0.065 in.)-diameter. As the leads from the thermocouples emerge from the tubes at the top of the canister, they are supported along the lower heater stem until they enter flexible stainless steel conduits. These flex conduits carry the leads to a thermocouple extension-wire transition junction near the top of the borehole. The type-K extension wire then goes to a ice point reference located in the instrumentation racks. Two additional thermocouples are to be located 180° apart at the level of the heater-element cold pin and terminals. The leads from these thermocouples also pass into the above flex conduits.

Four separate electrical-heating elements are to be suspended into the simulated waste canister (see arrangement shown in Figure 3). Each heating element is shaped in the form of a long hairpin. These elements are of a standard, commercially available type of construction. They are assembled with an 0.5-in.-diameter nickel alloy (Incoloy 800) sheath, mineral insulation, and a coiled central-resistance wire. Each leg of the hot section has a 96-in. "hot" length plus a 47-in. "cold" length and is terminated with a hermetically sealed high-temperature ceramic insulating bushing between the tubular sheath and the nickel cold pin. The heating element is supported from a nickel alloy collar brazed to each cold leg.

The total design load for the four heating elements is a maximum of 5,000 watts (normally 1250 watts per element). However, each element is capable of delivering up to the full 5,000 watts to maintain program power in the event of failure of one or more heater elements. Power levels over 5 kW are possible for a final overload test if borehole failure has not occurred after two years.

Several tests shall be performed to verify the quality of each heater element. These tests are:

(1) Radiographic examination to verify that the mineral insulation is free of metallic inclusions and voids, that the welds are sound, and that the resistance wire and cold leads are properly centered.

(2) Cold resistance check for continuity and to verify uniformity of resistance.

(3) To check that the insulation leakage current at 1500 volts is less than 6 milliamperes.

(4) Bench test under power for one hour before assembly into a canister.

(5) Eight hours operation at 5 kW per individual element while the canister assembly is installed in a simulated borehole.

The maximum heating-element sheath temperature has been calculated for the case of a single heating element energized at 5 kW when mounted in a 724°C canister. Emissivities of 0.8 for the sheath, 0.7 for the canister, and a geometry factor of 0.7 for the enclosed ring of heater elements lead to a predicted maximum temperature of 767°C for the heater sheath. The long "cold" length of the element passes through a heat plug to locate the terminal connections in a zone which is well isolated from these maximum temperatures.

Two power leads (to provide redundancy and a conservative current density) plus a voltage sensing lead (to provide for measuring the net downhole power and for monitoring lead condition) are attached to each cold pin of each heating element. The voltage sensing lead is attached at a point on the heater cold pin which is below the power lead attachments (see Figure 19).

Heater terminals are often trouble spots; therefore, particular care was taken to provide a conservative design for these connections. They must withstand ambient temperatures up to 200°C and a moist environment while maintaining their mechanical and electrical integrity over a long period of time. A nickel ring is to be crimped around the coldpin and the leads to provide a strong mechanical joint. To assure that oxidation products will not build up between the leads and the cold pin, this crimped joint is to be brazed with a copper/silver alloy. The brazed joint is wrapped with glass-woven tape and secured with a heat-shrink Teflon tube. The insulated joint is encased in a layer of silicone rubber (G.E. RTV-162) for waterproofing. This high-temperature silicone compound was selected because it cures without producing acetic acid.

A variety of lead wire constructions were evaluated for the original Stripa-heater design including solid or stranded wire, copper, nickel-plated copper, or alloy wires, as well as ceramic bead, sleeve type, or braided type insulation. The lead construction selected was stranded, #12 nickel-alloy wire with Teflon tape plus asbestos and Teflon-coated glass braid insulation (see element "B" in Table 11). This lead wire is rated for 600 volts operation at 250°C. The alloy was selected because it is more resistant than copper to corrosion at elevated temperatures. While the electrical resistance of the alloy is substantially

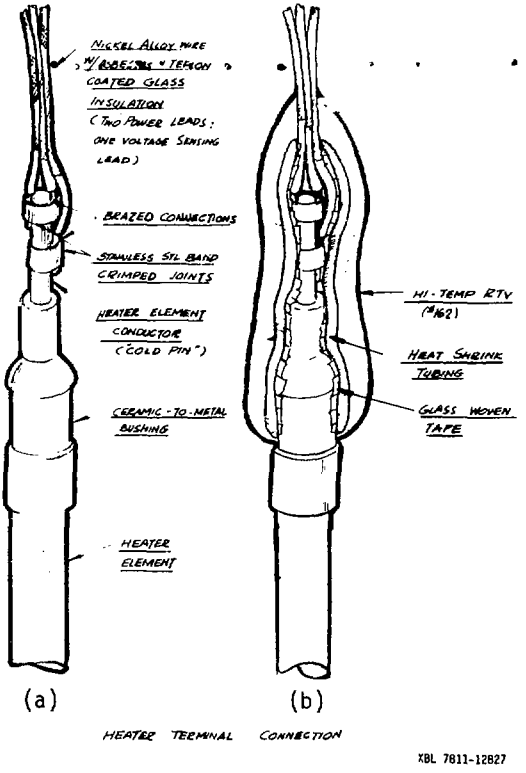

Figure 19. Typical Heating Element Connection in a) Bare Connection, b) Insulated Connection.

higher than that of copper, the power loss in the leads is negligible. The Teflon and braid insulation is compact, flexible, low in friction, and suitable for long life at elevated temperatures.

TABLE 11. Lead wire voltage drop.

Element	Wire Type	Insulation	Voltage drop at 5 kW
A	Copper 2-#12	Asbestos Teflon-glass	0.7
B	Ni-alloy 2-#12	Asbestos Teflon-glass	1.3
C	Ni-alloy 1-#12	Asbestos	2.4
D	Ni-alloy 1-#12	Ceramic bead	2.5

To verify the ability of this insulation to resist a high-temperature moist environment, a ten-meter length of the lead wire, with 110-volt a.c. applied, was placed in a 70°C salt solution for 72 hours, and then placed in a 70°C cupric-sulfate solution for 96 hours. In both cases the leakage from conductor to test container remained less than the minimum sensitivity (5 ma) of the instrumentation. For protection against mechanical abuse, all leads are to be encased in flexible stainless-steel conduits. These flexible conduits are anchored, to isolate them from strain, at a collar 4 inches above the heating element terminal.

Several of the original heater assemblies were operated in a simulated borehole for a minimum of 408 hours with 1,250 watts applied simultaneously on all four elements plus 24 hours of operation on each element singly at 5,000 watts. Typical temperatures reached were 540°C on the canister wall and 150°C at the heater element connection. All leads tested (see below) showed little or no heat effect; however, the ease of installation was markedly better for the asbestos Teflon-glass braid insulation.

The tubular heater-assembly stem (see Figure 20) is designed in two parts. The lower part, with heating elements and leads, is attached to the canister at the time of original assembly. The upper part of the stem is attached after the canister is lowered part way into the borehole. The demountable arrangement allows the heater assembly to be installed within a drift which has less than 17 feet of vertical clearance. This stem provides:

(1) Support for the heating elements.

(2) Support for the electrical leads.

(3) Support for the thermocouple leads.

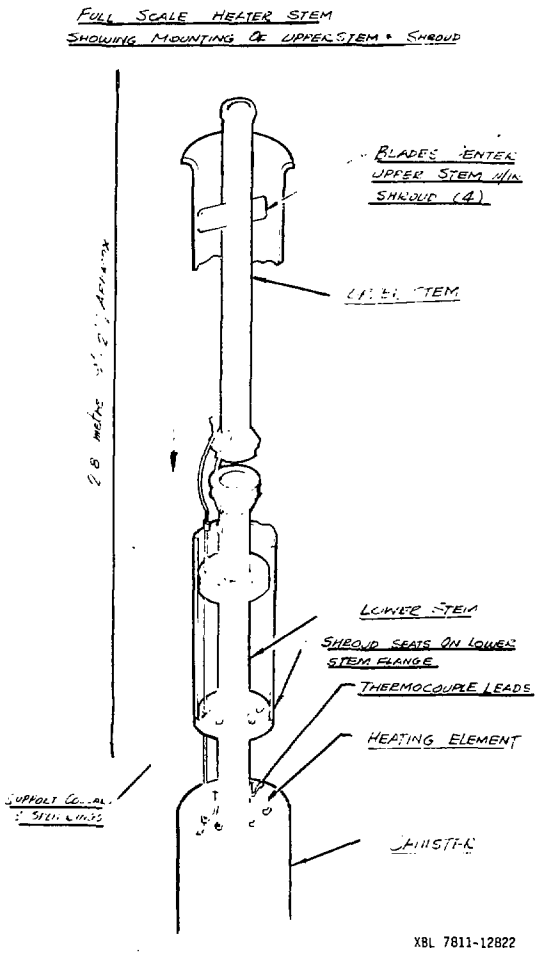

Figure 20. Full-Scale Heater Stem Showing Mounting of the Upper Stem and Shroud.

(4) Clearance for the optical-pyrometer view line.

(5) A means for supporting the canister as it is lowered into the borehole.

A ring-shaped thermal insulation layer (see Figure 21) is designed to rest on top of the canister to block convective heat transfer up the annular region between the tabular stem and the borehole. This heat plug is to consist of:

(1) A wire screen fastened to the top of the canister.

(2) A layer of wire-reinforced asbestos cloth fastened to the top of the canister.

(3) A 300-mm (12 in.)-thick layer of vermiculite -- a granular high temperature insulation -- poured into place after canister installation.

During normal heater operation a cylindrical plug is to be lowered into the tubular stem to prevent convective heat loss. When this plug is temporarily removed, a clear optical-pyrometer viewline will be available from the top of the borehole into the interior of the canister. This viewline intercepts a portion of one of the sheet metal spacers, which are positioned along the heating elements (see Figure 18), and the bottom of the canister.

At the top of the borehole, a metal collar is to be grouted in place to prevent surface water from entering the hole, and a concrete leveling collar is to be formed at the top of the boreholes to support the dry collar. Radial screws in the metal collar center the stem within the collar. Four struts, which are clamped onto the top edge of the collar, support the upper ends of four vertical guide tubes. The lower ends of these tubes terminate just below the thermal insulation layer. A borescope, a portable thermocouple probe, or a dewatering tube (described below) may be passed down these guide tubes into the annulus outside the canister and into the annulus outside the borehole liner.

Peripheral Heaters

The peripheral heaters (see Figure 22) are to be much simpler than either the full scaled heaters or the time scaled heaters. They include no downhole instrumentation or dewatering apparatus.

The Design Criteria include the following:

(1) Mounting in a borehole which is 1.5-in.-diameter x 21-ft-deep.

(2) Providing 1,100 watts of heat over a 14-ft-length, centered in the same plane as the center of the full scale heater.

(3) Providing a single heating element to mount inside a protective housing with provision for replacement.

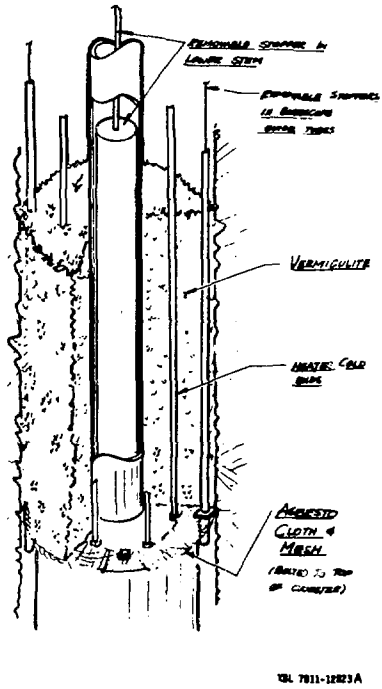

Figure 21. Details of Heat Plug for Full Scale Heater.

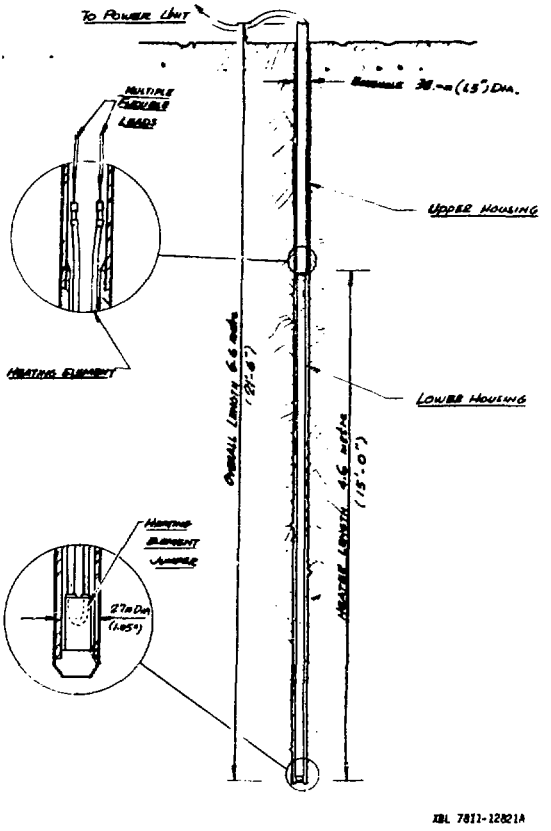

Figure 22. Peripheral Heater Installation.

(4) Estimating maximum borehole temperature as being 160°C depending upon the power scenario selected.

The peripheral heaters do not use a canister but do incorporate a protective housing which occupies the full length of the borehole. This protective mounting tube is made in two parts for installation where there is limited overhead clearance. The lower section is a type-304 stainless-steel pipe (3/4-in. nominal size) with a chamfered plug welded into the bottom and a collar having external threads welded to the top. This collar mates with an internally threaded collar which is welded onto the lower end of the upper tube. The upper tube is larger (1-1/4-in. nominal size) to provide clearance for the electrical heating terminals.

This style of heater assembly will use a single U-shaped heating element. This element is to be rated for operation at up to 1,500 watts and, in case of failure, it can be quickly replaced. It is similar to the heating elements in the full scale heater, except that the return bend is replaced by a cylindrical stainless-steel junction box into which the two legs of the "U" are welded. This change is required because the housing does not provide enough space to accommodate a "U" bend. Sheet metal discs are to be welded to the legs at four locations along their length to space them within the protective mounting tube. Each disc has two additional holes so that thermocouples could be inserted if necessary. These peripheral heater elements are expected to operate in a lower temperature environment than the full scale heaters and will require a "cold" length of only 12 inches to separate terminals from the hot zones.

The leads, connections, and protective flex conduit are similar to those described above for the full scale tests.

Time Scaled Heaters

A time-scaled heater (see Figure 23) is a miniaturized (approximately one-third scale) and simplified version of a full scale heater. There are thirteen time-scale heaters. All of these are identical except for the possibility of minor variations in length.

The Design Criteria include the following:

(1) Mounting in a borehole which is 5-in.-diameter x 35-ft-deep.

(2) Predicting the borehole temperature as being 400°C.

(3) Making sure that the heat is uniformly distributed over 30 inches of borehole length centered at 33.5 feet below the floor of the drift.

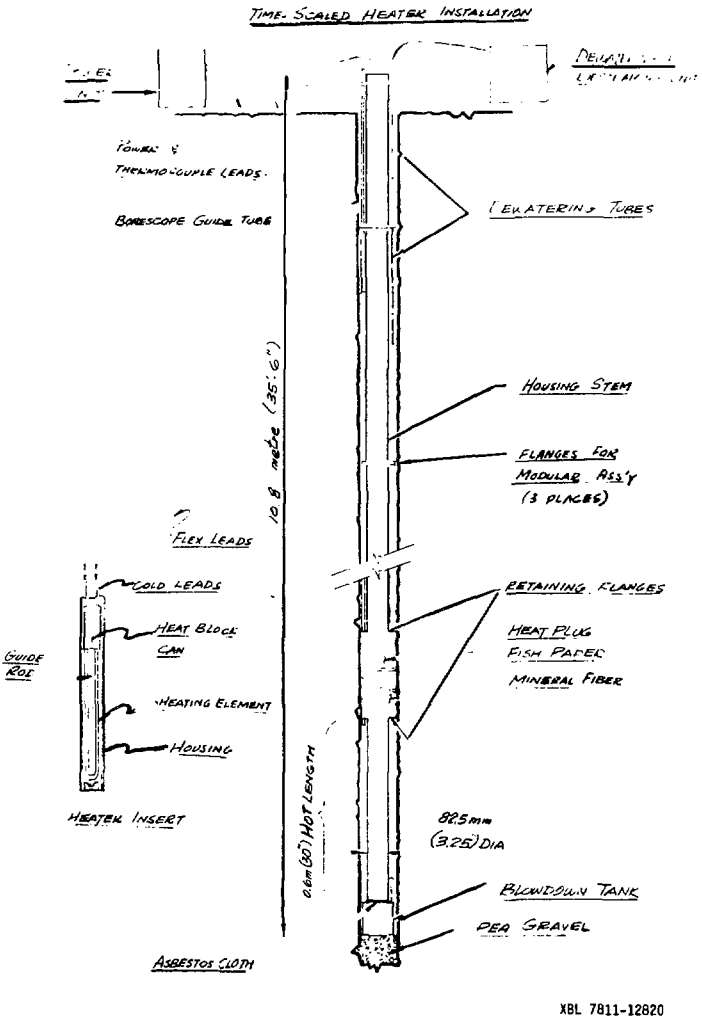

Figure 23. Time Scale Heater Installation.

(4) Using two heating elements for 1100-watt total load, with leads as for full scale heater.

(5) Designing for a test duration of three years.

(6) Minimizing heat loss up the borehole.

(7) Designing for installation in a drift having limited (23 feet) roof clearance.

(8) Designing for possible removal from the borehole.

(9) Providing thermocouple monitoring of the temperature of the protective heater housing.

(10) Providing equipment to remove water and steam from the annular space between cylindrical heater housing and the borehole and to measure their flow rates.

(11) Providing a means for optically inspecting the heated portion of the borehole with a borescope.

Although the time scale heaters are reduced-size simulators of the full scale heaters, the details of construction are somewhat different. For example, the time scale heater housing extends the full length of the borehole. This housing is designed to be made in a minimum of two sections of stainless steel tube 3.25 inches in diameter. These sections are to be bolted together by their welded end-flanges at the time of installation.

To accommodate out-of-straightness of the rock bore, the flanged joints will be joined with a flexible fastening system. Bellville (conical) spring washers are captured under the flange bolts. Under test these joints have provided for a misalignment of 0.5°. The lower end of the heater housing is closed by a welded plug which has a central recess to engage and center a rod on the heating element assembly. A removeable bellmouthed collar is provided at the upper end of the housing to prevent chafing of the electrical leads. To compensate for the fact that the center points of all time scale heaters lie in the same horizontal plane while the drift floor is rough and sloped, the length of the upper section of each heater housing may be tailored to suit its individual location.

To prevent heat loss up the annular space between the heater housing and the rock bore, an external insulating plug is provided on the heater housing above the "hot" zone. This insulating plug consists of a mineral fiber blanket wrapped around the tube and confined length-wise by two external flanges. To assure that the plug may be easily lowered into the rock bore, the fiber blanket is wrapped with a layer of "fishpaper" (electrical insulation) and is held

in a compressed state by adhesive tape. When the heaters are turned on, the fishpaper and tape burn off to allow the mineral wool to expand and make contact with the rock bore.

The thermocouple-dewatering and borescope-guide tubes are similar to those described for the full scale heater. However, sections of these tubes are welded to the individual sections of the heater housing. The housing flanges are keyed to assure that the tube centerlines are aligned. The thermocouples are inserted after the housing sections are joined. Two thermocouples are provided for monitoring the housing temperature adjacent the center of the "hot" section. One thermocouple is in each of the guide tubes. The thermocouples are the same as those described for the full scale heater.

The heating elements and their flexible leads are to be made into an assembly which can easily be lowered (by the leads) into the previously installed housing. The materials of construction for the leads, the heating elements, and their terminations are the same as for the full scale heaters.

The elements have a 30-in.-long "hot" section and an 18-in.-long "cold" section. They are each rated for 1500 watt operation but will normally be energized at 500 watts.

The "cold" lengths of the U-shaped heater elements pass through a stainless steel can, which blocks the loss of heat upward through the center of the housing. The interior of the can is filled with vermiculite and its removable top flange captures a heavy glass-cloth disk. The edge of the cloth will conform to the inside diameter of the housing to prevent air circulation around the loose fitting can. The heating elements are attached to the removable top flange of the can by collars brazed to the "cold" legs of the elements. A central vertical rod is welded to the bottom of the can and several stainless steel discs, with clearance holes for the rod and for the heating elements, are secured by cotter pins along the length of the rod. These discs will guide the heating elements within the housing. The central rod engages the bottom plug of the housing to center and support the heating element assembly.

Auxiliary Systems

There are four auxiliary systems proposed for use with the various types of heaters. These are:

(1) Borescope - 1/2-in. x 36-ft long for T.S. heaters
- 5/8-in. x 22-ft long for F.S. heaters.

(2) Optical pyrometer.

(3) Portable thermocouple probe.

(4) Dewatering pump.

Borescope

The borescope is an optical assembly for viewing the interior surface of a borehole. It can periodically be used, during the life of the tests, to inspect the heated wall of each of the full-scale and time-scale heater boreholes for evidence of decrepitation. The Stripa heater tests used a 1/2-in. O.D. borescope only; however, for the NSTF installation a larger diameter unit is recommended for the full scale heaters. This larger diamter unit will provide a more rugged assembly and an improved view of the critical full scaled borehole.

A borescope consists of a high intensity lamp, a prism, and a number of coaxial lenses -- all mounted in a stainless steel tube. The lamp is at the bottom of the assembly to illuminate the borehole wall. It is powered by a variable voltage power controller which plugs into the eyepiece at the top of the assembly. The prism is positioned to rotate the optical path 80^{o} so that it passes up through the lenses to the eyepiece at the top of the borehole. A camera adapter attached to the eyepiece allows a photographic record to be made.

The borescope can be rotated and raised or lowered within the guide tubes which are on the exterior of a heater assembly. These guide tubes end just below the layer of thermal insulation at the top of the heated zone. By moving the borescope, the scope's field of view can be translated along the length of the borehole and rotated about its axis to scan the portion of the borehole which is below the guide tube. Only a portion of the periphery is visible from each guide tube position since the canister itself occupies the center of the borehole.

To view the heated length of the time scale boreholes requires an optical path 10 m long. Therefore, the borescope assembly would be manufactured in several segments and these would be screwed together as they are lowered into the guide tubes. The full scale borescope would have fewer segments.

To make the unit useful for continuous observations within a 300^{0}C environment and for short observations in hotter surroundings, the lower section of the borescope tube should be silver plated and polished to create a highly reflective surface. A supply of a dry-nitrogen purge gas should be attached to the assembly near the eyepiece. This gas should exit near the lamp and mirror. The gas continuously cools the assembly. Additional cooling may be provided by a second purge-gas supply that flows through the annulus between the guide tube and the borescope.

Optical Pyrometer

A hand-held optical pyrometer may be used to periodically measure temperatures within the full-scale heater canisters. A pyrometer such as the pistol type unit made by Raytek of Mountain View, California may be used. Its temperature range is 350 to 700^{0}C. Its angle of view is 0.4^{o}.

To make a temperature measurement, the operator will temporarily remove a thermal plug which is suspended inside the stem of the heater assembly. This clears a view line into the center of the canister.

Portable Thermocouple Probe

The Stripa experience has shown that it is desirable to have a device that will allow a periodic survey of the temperature profile along the borehole wall, the canister wall, and for Hanford, the liner wall. No such device has been constructed; however, a conceptual sketch for one is shown in Figure 24. This unit would be similar in appearance to a borescope. It would be operated by lowering the pivoted thermocouple junction down through a borescope guide tube and then activating a push-pull rod to swing the junction out against the wall. By rotating the tubular assembly 180^{o} one can also sense the temperature of the opposing wall. By sensing the temperature of the canister at its mid-length, this moveable thermocouple can be calibrated against the fixed thermocouples which are part of the canister assembly. A second thermocouple could be fixed at the lower end of the probe. This second thermocouple would be able to sense the temperature of any water which might collect at the bottom of the borehole.

Dewatering Pump

Water leaking into a heater borehole can result in the generation of steam. The steam may escape or condense at some cooler portion of the borehole and thus result in a loss or redistribution of the intended heat load upon which the numerical modeling is based. There are, at present, no indications that natural water will be present in the boreholes of the NSTF. However, experience during the mining operation may change this conclusion. Also, water used during the mining and borehole drilling may be stored in the rock and then leak back into the boreholes during the heater test period. The conservative approach would be to design a system to remove water in the form of both liquid and steam. The equipment used in Stripa was designed to operate on either liquid or steam; however, there would undoubtedly be a period when both phases require pumping. It seems probable that any liquid removed would represent a negligible heat loss. On the other hand, steam (with its higher enthalpy) could easily represent a significant loss.

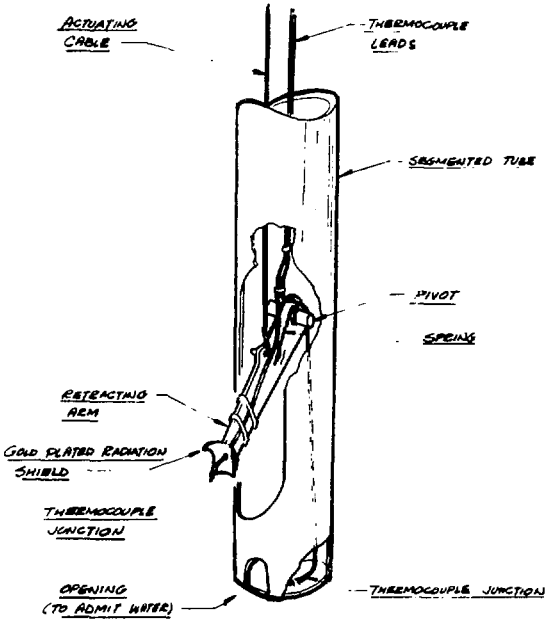

Figure 24. Portable Thermocouple Probe.

On each heater assembly, one of the borescope guide tubes can be adapted for removing steam. Both steam and air are drawn from the borehole through this tube. The guide tubes extend from the top of the hot zone (just below the heat plug) up to the top of the borehole. At this top end another tube is attached. The opposite end of this extension tube may be attached to the inlet of a steam condenser which would in turn be connected into an evacuated reservoir. The thermal insulation layer at the top of the canister has a sufficient impedance to the inflow of air to maintain a negative static pressure in the borehole. This characteristic was demonstrated in a mock-up of both the full scale and the time scale desteaming. Both guide and extension tubes may be wrapped with thermal insulation and have an electric heating tape threaded through their full length, or a hose with an integral heater (new commercial product) may be used. These heaters require about 18 watts per foot to prevent the steam from condensing and refluxing in the tubes. An auto transformer should be provided for the heated line to adjust the steam temperature at the entrance to the condenser to slightly above the boiling point. This will assure that the steam is not condensing in the line and refluxing.

The technique for liquid removal may be somewhat different for the full scale heaters than for the time scale heaters due to the difference in their borehole depths. The full-scale borehole depth of 18 feet allows the removal of water by direct suction. The 35-foot depth of the time scale boreholes requires a different technique. Liquid removal from the relatively shallow, full-scale heater borehole may be accomplished with a simple suction tube passing from the collection barrel to the bottom of the borehole. A fine mesh screen should protect the inlet of the tube. Liquid removal from the time-scale heater borehole may be accomplished with two tubes as shown in Figure 25. This technique was used at Stripa. An individual pumping unit was used for each heater borehole in that scheme; however, a change to a centralized pumping system for each of three heater experiments is being proposed for the NSTF. This up-hole equipment has not been designed and its design can probably be deferred until a definitive assessment can be made regarding the probable quantity of water to be collected.

Calipers and Weighpan

Two borehole caliper assemblies and a decrepitation weighpan were installed on two of the Stripa time-scale heaters. Initial experience with these devices has not been encouraging and they are not being recommended for the NSTF heaters. Sketches of these devices are included (Figures 26 and 27) for reference only.

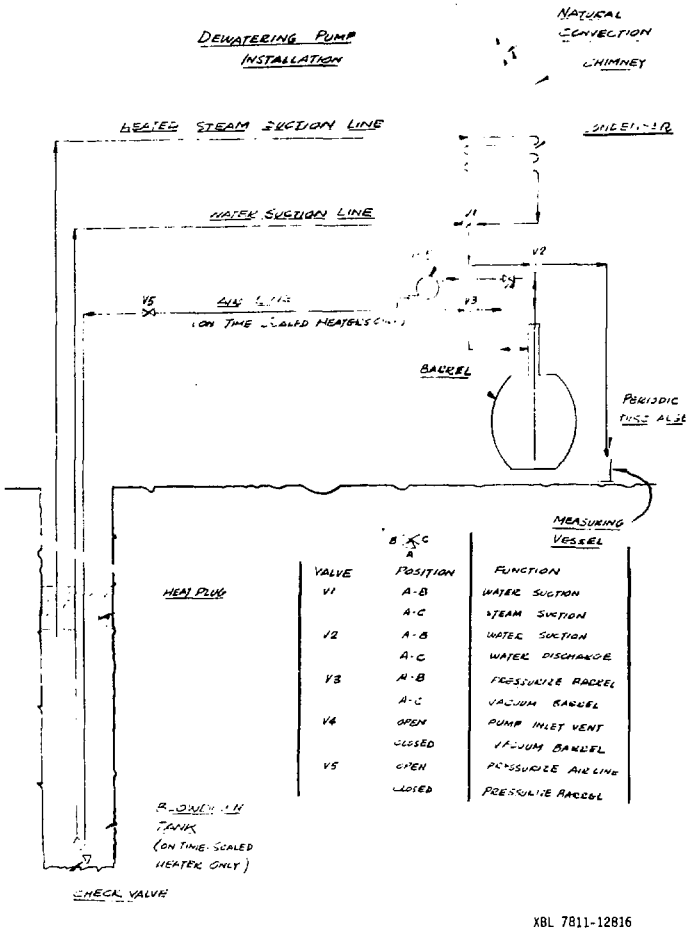

Figure 25. Schematic of Dewatering Pump Installation.

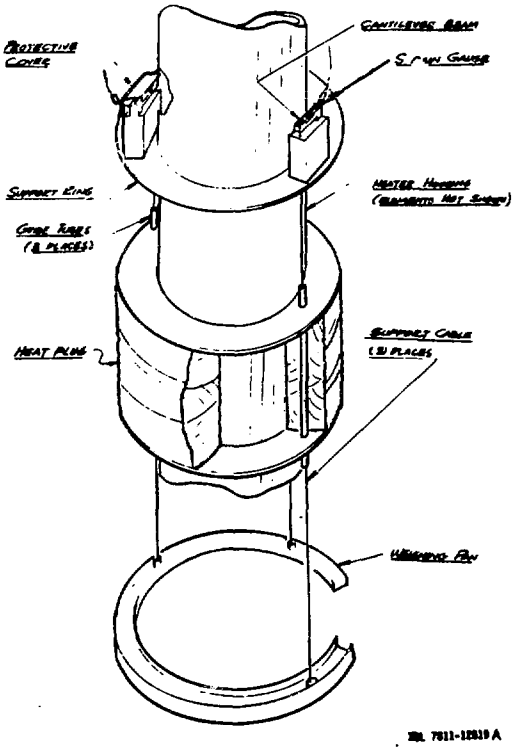

Figure 26. Caliper Assembly Installed in the Time Scale Heater Borehole.

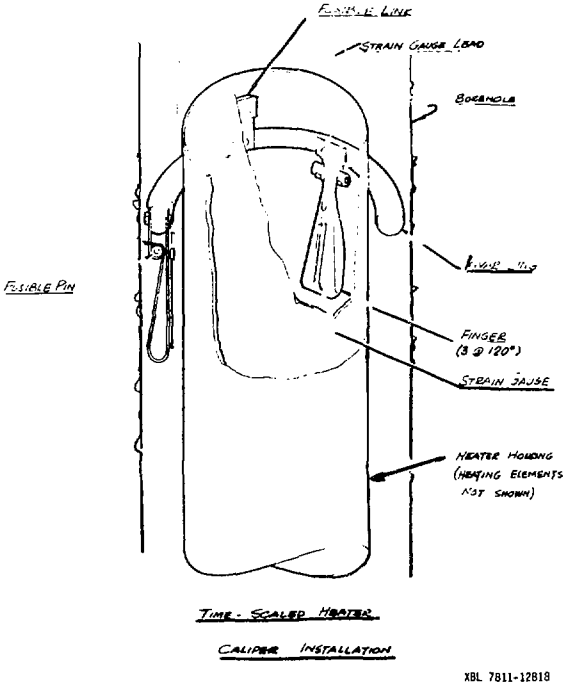

Figure 27. Weighing Pan Assembly Installed on the Time Scale Heater.

Electrical Heater Controllers

Electrical heater controllers are required for two full-scale heaters, sixteen peripheral heaters, and thirteen time-scale heaters. During earlier meetings between LBL and RHO, both parties agreed that all heater controllers were to be powered from a 240-volt, 3-phase, delta-connected power source. At the Hanford meeting on April 5, 1978, between LBL, Terra Tek, and Rockwell personnel, Rockwell proposed using a 208/120 volt, 3-phase, Y-connected power system. Heater elements have, therefore, been specified to operate at maximum power outputs with voltage settings of 208-volt a.c. from the power controllers. Table 12 shows the various heater voltage settings to be provided by the controller for designated heater power outputs.

TABLE 12. Heater element operating power and voltage.

	Full Scale #1	Full Scale #2	Peripheral	Time Scale
Heater Assemblies per Project	1	1	16	13
Heating Elements per Assembly	4	4	1	2
Maximum Power per Element (kW)	5	5	1.5	1.5
Maximum Voltage Setting (VAC)	208	208	208	208
Normal Power (kW), All Elements Energized	1.25	0.5	1.0	0.5
Normal Voltage (VAC), All Elements Energized	104	66	170	120
Normal Power (kW), One Element Energized	5	2	1.0	1.0
Normal Voltage (VAC), One Element Energized	208	132	170	170

Following the philosophy used in the Swedish experiment, each full scale heater will have four heater elements with each heater element driven and monitored by its own power controller. Under normal operation, the power load will be shared by the four elements and associated controllers. Each element and controller is designed to handle the full heater power in the event of failure of up to three heater elements and/or controller channels. Each controller is also a modular unit capable of replacement within a few minutes. By selecting

adequately sized wiring, circuit breakers, and power sources to the controllers, all heater elements can be turned up to provide a maximum, full-scale heater canister power-output of up to 20 kW for rock and/or canister destruction tests at the end of the experiment. A total of eight active, plus at least two spare, full-scale heater controllers should be provided.

The peripheral heaters are single element heaters. In the Swedish experiment, four peripheral heaters are powered in parallel by a single controller chassis capable of over 5 kW. However, independent monitor chassis were used for each peripheral heater to monitor current, voltage, and power. It seems apparent that there is little or no savings in making a single, large-power controller for each set of four peripheral heaters and providing independent monitor chassis for each heater. LBL has proposed to Rockwell personnel, at the meeting at LBL on September 14, 1978, that the heater controller capability should be combined into each of the individual monitor chassis with each controller capable of 1.0 to 1.5 kW. By doing this, the peripheral heater controller/monitor chassis can be duplicates of the controller chassis used in the time scale experiment. A total of sixteen active, plus at least two spare, controllers should be provided for the peripheral heaters.

The time-scale heater canisters each contain two heater elements, and, like the full scale heater, each element is controlled and monitored by an independent controller. Under normal operation both elements and their associated controllers share the burden of supplying canister power. Each element/controller set is capable of supplying full heater power in the event of emergency. Each controller is constructed as a modular chassis for ease of replacement. Twenty-six controllers, plus at least two spare units, should be provided for the thirteen time scale heaters.

The various controllers follow the same basic hardware philosophy. Each unit contains an autotransformer as a voltage source for the heater elements. Four independent, electrical transducers and signal conditioners are provided to monitor autotransformer output voltage, the voltage drop directly across the heater elements, current through heaters, and heater power. The redundancy of independent current, voltage, and power transducers are used to provide a cross-check of the power dissipated in the heater elements. Operational amplifiers are used as buffers between the transducer/signal conditioner outputs and lines that drive analog panel meters, digitial panel meters, data logger inputs, and computer multiplexer inputs.

Several other controller types have been discussed as possible alternatives to the direct autotransformer controller used in Sweden. These include:

(1) A fixed transformer with switched taps to provide coarse voltage adjustment and a smaller autotransformer used in a "Buck/Boost" configuration to provide fine adjustment.

(2) Phase-controlled SCR circuits.

(3) Zero cross-over firing SCR circuits.

(4) Various types of adjustable, d.c. power suppliers.

Of these, the two that seem the most promising are the "Buck/Boost" circuit (1) and the "Zero cross-over firing SCR" (3). The latter does cause some complexity in monitoring the power dissipation in the heater elements.

In July 1978, two block diagrams (29X1385 - B1 and 29X1384 - B2) outlining full-scale and time-scale heater control configurations were delivered to RHO. At a meeting on September 14th at LBL between electronics personnel from Rockwell and the Field Systems Group at LBL, we reviewed the available print packages of controller systems used in the Swedish project. A set of full-scale, peripheral, and time-scale heater controller prints were supplied to Rockwell. These included 51 electrical and mechanical prints for the full scale controller and monitoring equipment, 69 electrical and mechanical prints for the peripheral heater controller and monitoring equipment, and 6 electrical prints of the time-scale controller and monitoring equipment. Drafting of the time scale equipment has not been completed, and there are some updates to be made on the full scale and peripheral documents.

Electronics racks containing the heater controller and instrumentation electronics will be housed in two buildings within the experiment drift. In February 1978, LBL recommended that these structures be sized to have internal dimensions of 10-feet wide, 35-feet long, and 10-feet high with the floor elevated about 3 feet above the drift floor. One structure was to be located at the time scale experiment and the other at the full scale experiment. After our experience with the crowded instrumentation buildings in Sweden, and considering the increased amount of equipment to be installed at Hanford, we asked that the full-scale instrumentation building be increased in length to 45 feet. In July 1978, five LBL drawings (29X1304 L-1 and 29X1303 L-2 through 5) were given to RHO outlining these dimensions, door locations, and various other internal configurations. At the July 31/August 1 meeting at Hanford, RHO and Vitro made some further suggestions for improving the structures, including the use of

elevated computer-room-type flooring. LBL reviewed the Vitro drawings of the buildings and made suggestions about: locations of HVAC equipment, door locations, locations for electrical outlets, cable tray and conduit locations, etc. LBL has continued communications with Vitro and RHO on details of these subjects since that meeting.

VI. INSTRUMENTATION AND DATA ACQUISITION SYSTEM
M. McEvoy and G. Binnall

Instrumentation was proposed that would determine the mechanical and thermal response of basalt to the full- and time-scaled heater tests. These instruments, which are listed below, include thermocouples, stressmeters, and extensometers similar to those currently being used by LBL in Sweden:

(1) Thermocouples. Temperatures will be measured using type-K (Chromel-Alumel) thermocouples with Teflon insulation for temperatures below 250°C and with Inconel sheath for temperatures above 250°C.

(2) U.S. Bureau of Mines Borehole-Deformation Gauges. These gauges measure borehole diameter deformation in three equally spaced rotations normal to the borehole axis. These instruments use strain gauges as the electrical transducer and therefore require signal conditioning amplifiers as part of the data acquisition system. Each unit must also be temperature calibrated, monitored, and have output readings corrected for the operating temperature.

(3) Vibrating Wire Stressmeters. These instruments measure borehole diameter deformation and are used in orthogonal pairs. The heart of this instrument is a vibrating wire whose vibration frequency is a function of the wire tension which varies as a function of the deformation of the borehole. A special frequency-counter type data-logger is used to digitize the output of these gauges. Each gauge output reading must also be corrected for temperature variations.

(4) Borehole Extensometers. These instruments measure rock movement over the full or partial length of a borehole in a direction parallel with the borehole. The Swedish experiment used four-anchor extensometers. Each anchor's displacement is referenced to the collar of the hole and is monitored by a linear DCDT transducer (a special LVDT transducer containing hybrid circuits to provide signal conditioning). Temperatures are monitored along the extensometer borehole (usually at anchor points) to provide rock temperature data and to be used to correct for thermal expansion of the "super invar" rods used in the extensometers.

On December 1, 1977 LBL personnel and a representative from Terra Tek met with Rockwell personnel to more clearly define the Hanford heater-test experiment. The result of this meeting and other conversations was the description of a NSTF that would include two full-scale heater experiments and a time-scaled heater experiment. One of the full scale heaters was to operate at 5 kW and the other at 2 kW, each to be surrounded by eight 1-kW peripheral heaters. The time

scaled experiment was to use nine 1-kW heaters arrayed in three rows each having three heaters. After two years of operation, four additional time-scaled heaters were to be interspersed in this array for a total of thirteen heaters.

With the above criteria in mind, a rough instrumentation proposal was compiled in January 1978 by Terra Tek that included an instrumentation count of 390 rock temperature-monitoring thermocouples, 33 USBM gauges with three channels per gauge, 35 vibrating-wire stressmeters, and 35 four-point extensometers. This instrumentation count was changed in April 1978 to 712 rock instrumentation thermocouples, 74 USBM gauges requiring 222 data channels, 148 vibrating-wire stress meters, 279 channels of three- and four-anchor extensometers, and other block motion transducers. To this count LBL added 130 heater thermocouples and 190 current, voltage, and power monitoring signals from the heater controllers.

With a total of more than 1681 data-acquisition channels required, LBL and Terra Tek developed preliminary block diagrams for the instrumentation Data Acquisition Systems (DAS). Basically the DAS for the two full-scale experiments and time scale experiment included ten 96-channel Ice-Point References (IPR) for thermocouples, three general-purpose data loggers, strain-gauge signal conditioning circuits for 222 channels of USBM gauges, and custom data-loggers for the vibrating wire stressmeters.

A revision of borehole instrumentation requirements in August 1978, by Terra Tek, under LBL P.O. #309902, lowered the required number of DAS channels from 1681 to 1576 channels. The initial, basic DAS block-diagrams are still generally valid; however, there are changes that should be considered as a result of LBL's experience in Sweden.

In the case of IPR units, each output should be provided on two connectors, one to go to the data logger equipment and the other to go to the computer multiplexer input. This will eliminate the signal splitter chassis required in Sweden. Each of the connectors should provide 8 or 16 signal outputs so that the 8-channel computer multiplexer connectors can be cabled conveniently. The twin modulo-eight connectors hould be provided even at the expense of fewer thermocouple channels per IPR chassis. A good compromise might be to drop to as few as 64 thermocouple channels per IPR with an additional four or more thermocouple channels for IPR-checking circuits.

LBL proposed an architecture for a DAS for the NSTF including requirements for a spent fuel facility, estimated its cost including test equipment and spares, and recommended how to meet the early turn-on requirements and general delivery schedule. The system was designed to acquire and digitize data from each of the

1576 channels at 15-minute intervals. Acquired data is logged on magnetic tape, converted to engineering units, smoothed, checked for alarm conditions, and stored on a local disc file. The DAS also provides the capability of calibrating the instruments on-site. Real-time graphic displays facilitate examination of the acquired data and aid in detecting and diagnosing problems. Predicted temperature, displacement, and stress data will also be maintained on a local disc file. Displaying both predicted and actual results together accentuates unexpected results. A means of rapidly displaying data from the 1576 sensors is required so that one may periodically examine the acquired data to detect faulty sensors or data acquisition hardware.

A Modular Computer Systems' Mod Comp IV/35B was proposed as the basis for the DAS. The proposed system configuration is shown in Figure 28 and detailed in a Department of Energy 1830 format and a "Functional Specifications of the Data Acquisition System" that LBL provided to Rockwell. The 1830 provided justification for the "Acquisition of Automatic Data Processing Equipment and Sole Source Procurement." This system was proposed to: utilize off-the-shelf remote analog I/O processors; maintain compatibility with the software developed for the Swedish system thus reducing software development costs; and provide memory expansion capability. Two Grinnell color-graphics terminals were selected to provide more visual and meaningful displays to the experimenters and experiment operators. LBL is currently using this graphics system together with high-level thoroughly documented graphics software from Tektronix. A Versatec Model 1200A printer/plotter was selected for hard copy. The Versatec plotter is connected to the Grinnell system to provide a hard copy device without requiring the reprocessing of the displays by a CPU. The printer/plotter also functions as a line printer which greatly facilitates the software development effort. Computer data will be logged onto magnetic tape at 15-minute intervals. Data loggers will print out at a six-hour sampling rate. Two nine-track tape drives were selected with raw data being logged on one tape drive. The second tape drive provides a backup in case of failure of the first. Two discs support a large data base that includes the operating system, application software, collected and predicted data for processing and display, calibration data, and engineering conversions. A third disc is provided for ongoing software development, maintenance, and as a spare drive for reliability. Paper tape is provided for entering computer diagnostics. An uninterruptible power supply will be used to protect against short power outages. Redundant computer peripherals, raw-data log-tapes, a file save/reload feature, and back-up data loggers are provided to minimize data loss caused by any single failure.

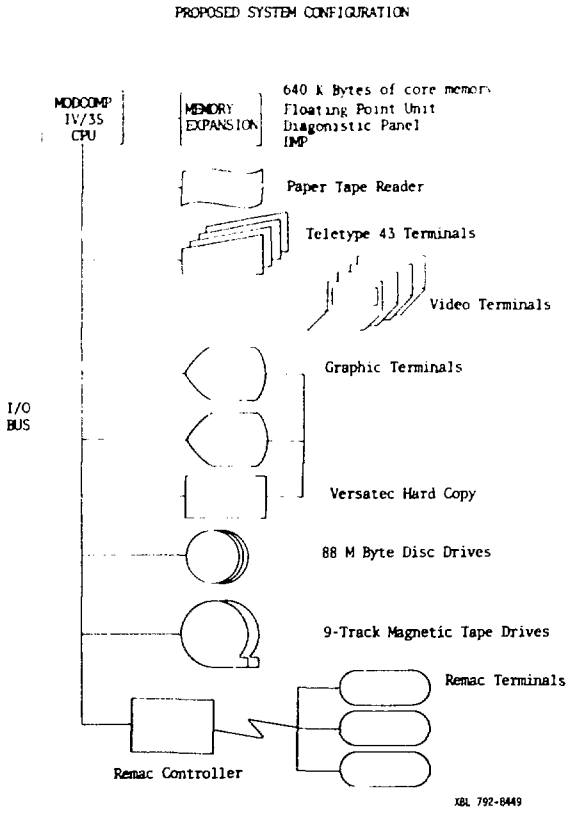

Figure 28. Proposed Data Acquisition System Configuration.

The computer system will be housed in a computer room that will be constructed underground near the heater experiments. Remote data-acquisition units (REMACs) will be housed in instrumentation sheds that will be constructed immediately adjacent to both the full-scale and the time-scaled heater experiments. LBL proposed a room layout, lighting, floor, power layout and emergency lighting for the enclosure for the computer and instrument electronics. The lighting will be dimmable, and battery-operated emergency lights will be provided. Smoke detectors, a halon fire-extinguisher system, and a power interlock system will provide fire protection. Two outside telephone lines will be provided for both safety reasons and for off-site data links. An intercom system will be provided between the computer room and each instrumentation shed to facilitate instrument calibration and troubleshooting. Drinking water and restroom facilities will be available. Temperature in the NSTF will be controlled to remain 15 to 25°C during installation and 10 to 40°C during operations.

LBL, together with Rockwell and Vitro Engineering, determined the requirements for normal power, standby power, uninterruptible power, and emergency power. A power interlock system, local audible alarms, and an automatic telephone dialer will be provided to give warning in the event of: computer power outages; computer's central processor malfunction; instrumentation-shed power outage; a smoke detector being activated; or heater power outage.

Several new data-logging systems have become available in the last year and a survey of the market should be made to pick systems that best match the project requirements. LBL has investigated the new Acurex Autodata-twenty for the Hanford project; however, there are several other units which should also be considered. Configurations and limitations of some alternate data loggers will change the DAS block diagram configuration, and may even effect the instrumentation house rack and table layouts. Any data logger selected must have a sufficiently sophisticated alarm capability to continuously monitor upper- and lower-limit set points on thermocouple channels and heater-power-controller monitor channels. A custom-designed alarm system similar to that used in Sweden should be designed as an interface to the alarm outputs of the selected data loggers.

LBL engineers conferred with Rockwell and Vitro engineers both at meetings at Hanford and with numerous telephone calls. This provided information needed by Vitro engineers to complete Title-One design and to start Title-Two design for NSTF. LBL provided the following specifications and drawings to Rockwell:

(1) Specifications:

RTEN 78-1	Specification for the Hanford NSTF Computer Enclosure.
RTEN 78-2	Requirements for the Instrument Enclosure. (HVAC)
RTEN 78-3	Critique of Vitro Engineering's one line electrical drawings, SK-6-303.
RTEN 78-4	Critique of Vitro Engineering drawings SK-6-304, SK-6-305, and SK-6-306.

(2) Drawings:

20Y5710 -	Power distribution.
20Y5700 -	Control room breaker panels.
20Y5694 -	60 Hz and 24v DC power panel.
20Y2954 -	Data acquisition one line, Sweden.
20Y5524 -	+24v DC power panel, and interlock, Sweden.
20Y5503 -	+24 DC surface interlock panel, Sweden.
20Y5680 -	Data acquisition complex floor plan and power distribution.
20Y5594 -	1 of 1 and 2 of 2 Westinghouse bus sheet.
20Y5820 -	Interlock system block diagram.

At Vitro's request, LBL reviewed and provided comments on Vitro engineering drawings and specifications.

A preliminary Quality Assurance (QA) plan was drawn up for the DAS and was integrated into the overall LBL QA plan for the NSTF.

VII. REFERENCES

Agapito, J. F. T., Hardy, M. P., and St. Laurent, L. P., 1978. Geo-engineering Review and Proposed Program Outline for Structural Design of a Radioactive Waste Repository in Columbia Plateau basalts. Rockwell Hanford Operations, Report RHO-ST-6.

Ayatollahi, F. S., 1978. Stress and Flow in Fractured Porous Media. Ph.D. Thesis, Department of Material Science and Mineral Engineering, Berkeley, University of California.

Bath, K. J., Wilson, E. L., and Peterson, F. E., 1974. SAPIV, A Structural Analysis Program for Static and Dynamic Response of Linear Systems. Berkeley, College of Engineering, University of California, Report EERC 73-11, June, 1973, Revised April 1974.

Carlsson, Hans, 1978. Stress Measurement in the Stripa Granite. Berkeley, Lawrence Berkeley Laboratory, LBL-7078.

Carslaw, H. S., and Jaeger, J. C., 1959. Conduction of Heat in Solids. Oxford University Press.

Chan, T., and Ballentine, L. E., 1971. The Energy Distribution of Electronic States in a Liquid Metal. Physics and Chemistry of Liquids, v. 2, p. 165.

Chan, T., and Cook, N. G. W., 1979. Calculated Thermally Induced Displacements and Stresses for Heater Experiments at Stripa. Berkeley, Lawrence Berkeley Laboratory, LBL-7061.

Chan, T., Cook, N. G. W., and Tsang, C.-F., 1978. Theoretical Temperature Fields for the Stripa Heater Project. Berkeley, Lawrence Berkeley Laboratory, LBL-7082.

Chan, T., and Remer, J. S., 1978a. Preliminary Thermal and Thermomechanical Modeling for Near Surface Testing Facility Heater Experiment at Hanford. Berkeley, Lawrence Berkeley Laboratory, LBL-7069.

_____,1978b. Semi-Analytic Thermal Calculations for Arrays of Nuclear Waste Canisters Buried in Rock. Presented at American Geophysical Union 1978 Fall Meeting, San Francisco, December 4-8, 1978. Abstract T75, Trans. Am. Geophys. Union, v. 59, p. 1189.

Cook, N. G. W., and Hood, M., 1978. Full-Scale and Time-Scaled Heating Experiments at Stripa: Preliminary Results. Presented at seminar on In Situ Heating Experiments in Geological Formations, Stripa, Sweden, September 12-15, 1978.

Cook, N. G. W., and Witherspoon, P. A., 1978. In-Situ Heating Experiments in Hard Rock: Their Objectives and Design. Presented at seminar on In Situ Heating Experiments in Geological Formations, Stripa, Sweden, September 12-15, 1978.

Department of Energy, 1978. DOE 1830 Appendix Proposal for Radioactive Waste Proposal Research Program Computer System. Submitted by LBL in September, 1978.

Duvall, W. I., Miller, R. J., and Wang, F. D., 1978. Preliminary Report on Physical and Thermal Properties of Basalt, Drill Hole DC-10, Pomona Flow --Gable Mountain. Earth Excavation Institute, Colorado School of Mines, Report RHO-BWI-C-11.

Ekren, E. B., Dinwiddie, G. A., Mytton, J. W., Thordarson, W., Weir, J. E. Jr., Hinrichs, E. N., and Schroeder, W., 1974. Geologic and Hydrologic Considerations for Various Concepts of High-level Waste Disposal in the Coterminous U. S. U. S. Geol. Survey open-file report p. 74-158.

Gale, J. E., Taylor, R. L., Witherspoon, P. A., and Ayatollahi, M. S., 1974. Flow in Rocks with Deformable Fractures in Proceedings Int. Symposium on Finite Element Methods in Flow Problems, Swansea, United Kingdom. University of Alabama at Huntsville Press.

Goodman, R. E., 1976. Methods of Geological Engineering in Discontinuous Rocks. West Publishing Co., St. Paul.

Goodman, R. E., Taylor, R. L., and Brekke, T. L., 1968. A model for the Mechanics of Jointed Rocks. Jour. Soil Mechanics and Found. Division, ASCE, v. 94, no. S.M. 3.

Jackson, J. D., 1975. Classical Electrodynamics., Second Edition. Wiley, New York.

Haimson, B. C., 1978. Report on Hydrofracturing Tests for In Situ Stress Measurements, Near Surface Test Facility, Hole DC-11, Hanford Reservation. Prepared for Lawrence Berkeley Laboratory, September, 1978. Appendix of this report, under separate cover.

King, M. S., 1978. Microseismic Detection System for Heated Rock. Submitted to LBL, August, 1978. Appendix of this report, under separate cover.

Kurfurst, P. J., Hugo-Persson, T., and Rudolf, G., 1978. Borehole Drilling and Related Activities at the Stripa Mine. Berkeley, Lawrence Berkeley Laboratory, LBL-7080.

Martinez-Baez, F., and Amick. E. H., 1978. Thermal Properties of Gable Mountain Basalt Cores, Hanford Nuclear Reservation. Berkeley, Lawrence Berkeley Laboratory, LBL-7038.

Morrison, F., 1978. Monitoring Rock Property Changes Caused by Radioactive Waste Storage Using the Electrical Resistivity Method. Proposal from the University of California to LBL, May 1978. Appendix of this report, published under separate cover.

Morse, P. M., and Feshbach, H., 1953. Methods of Theoretical Physics. McGraw-Hill, New York.

Nelson, P., 1977. Borehole Logging for Swedish Waste Storage Program - Status Report. Memorandum to P. A. Witherspoon, July, 1977. Berkeley, Lawrence Berkeley Laboratory.

Nelson, P. and Doe, T., 1978. Proposed Geophysical and Hydrological Measurement at NSTF, Hanford. Memorandum to Lawrence Berkeley Laboratory, May, 1978. Appendix of this report, under separate cover.

Noorishad, J., Witherspoon, P. A., and Brekke, T. L., 1971. A Method for Coupled Stress and Flow Analysis of Fractured Rock Masses. Berkeley, Department of Civil Engineering, University of California, Publication no. 71-6.

Presnall, D. C., Simmons, C. L., and Porath, H., 1972. Changes in Electrical Conductivity of a Synthetic Basalt During Melting. Jour. Geophysical Research, v. 77, no. 29, p. 5665-5672.

Rockwell Hanford Operations, 1978. In Situ Heater Experiment Plan. Unpublished document, July 1978.

Sackett, S., 1978. New Version of SAP4. Unpublished Memorandum, February 1978. Livermore, Lawrence Livermore Laboratory, MDG 78-14.

Terra Tek, 1978. Borehole Instrumentation Layout for Hanford Near-Surface Test Facility. Submitted to Lawrence Berkeley Laboratory in August, 1978. Appendix of this report, under separate cover.

Thorpe, R., 1978. Suggestions for Characterization of the Discontinuity System at Hanford. Memorandum, Lawrence Berkeley Laboratory, May, 1978. Appendix of this report, published under separate cover.

Witherspoon, P. A., and Degerman, O., 1978. Swedish-American Cooperative Program on Radioactive Waste Storage in Mined Caverns. Berkeley, Lawrence Berkeley Laboratory, LBL-7049.

U.S.GPO:1979-689-058(F)60